Attosecond Coherent Control of Symmetry Breaking and Restoration in Atoms and Molecules

INAUGURAL-DISSERTATION

TO OBTAIN THE ACADEMIC DEGREE
DOCTOR RERUM NATURALIM (DR. RER. NAT.)

SUBMITTED TO
THE DEPARTMENT OF BIOLOGY, CHEMISTRY AND PHARMACY
OF FREIE UNIVERSITÄT BERLIN

BY
CHUNMEI LIU
FROM SHANXI, CHINA

2019

This work was prepared under supervision of

PROF. DR. BEATE PAULUS (FREIE UNIVERSITÄT BERLIN)

PROF. DR. JEAN CHRISTOPHE TREMBLAY (UNIVERSITÉ DE LORRAINE)

from

SEPTEMBER 2015 UNTIL MAY 2019

1. Gutachter	PROF. DR. BEATE PAULUS
2. Gutachter	PROF. DR. JEAN CHRISTOPHE TREMBLAY
Date of Defense	July 3rd, 2019

Abstract

Symmetry is a fundamental phenomenon in science, and symmetry breaking is often the origin of subsequent processes which are important in chemistry, physics and biology. As is well-known, a laser pulse can break the electronic symmetry in atoms and molecules by creating a superposition of electronic eigenstates with different irreducible representations, which typically initiates attosecond ultrafast charge migration.

In the first part of this dissertation, an original theory of coherent laser control is proposed to induce the symmetry restoration of the electronic structure in atoms and molecules after symmetry breaking, with application to the oriented benzene molecule and to the ^{87}Rb atom. Four different strategies are proposed and corresponding sufficient conditions for symmetry restoration are derived analytically. The numerical and analytical results agree perfectly with each other. Meanwhile, the theoretical predictions for the ^{87}Rb atom have been confirmed by experimental partners in Japan, by means of high contrast Ramsey interferometry with a precision of about three attoseconds.

The second part is devoted to the electronic flux during charge migration in oriented benzene molecule. Two different patterns of adiabatic attosecond charge migration are investigated by laser induced preparation of two different non-aromatic superposition states. From the knowledge of the time-dependent many-body wave functions as a linear combination of many-electron wave functions obtained from conventional quantum chemistry calculations, we derive expressions for the time-evolution of the one-electron density and the electronic flux. This allows to specify the number of electrons flowing during a given charge migration process, together with the mechanism of charge migration.

In conclusion, this dissertation shows, for the first time, that the symmetry of electronic structure in atoms and molecules can not only be broken but also be restored by means of simple laser pulses. The coherent control strategies require strict control over the time-dependent phases of electronic wave functions. In practice, the precision required is few attoseconds - much shorter than the timescale of charge migration in such systems. The analysis of charge migration indicates that similar superposition states may lead to quantitative differences in the number of electrons flowing.

Kurzzusammenfassung

Symmetrie ist ein fundamentales Phänomen in der Naturwissenschaft, und Symmetriebrechung kann bedeutende Folgeprozesse in der Chemie, Physik und Biologie auslösen. Insbesondere kann die elektronische Symmetrie von Atomen und Molekülen bekanntlich durch einen Laserpuls gebrochen werden, und zwar durch die Erzeugung einer Superposition von elektronischen Zuständen mit verschiedenen irreduziblen Darstellungen - dies bewirkt dann typischerweise ultraschnelle Ladungsmigration auf der Attosekundenzeit-skala.

Der erste Teil dieser Dissertation entwickelt eine grundlegende Theorie der kohärenten Laserpuls-Kontrolle mit dem Ziel der Wiederherstellung der elektronischen Symmetrie in Atomen und Molekülen nach Symmetriebrechung, mit Anwendungen auf das orientierte Benzolmolekül sowie auf das ^{87}Rb Atom. Es werden insgesamt vier Strategien zur Wiederherstellung der Symmetrie vorgestellt, wobei hinreichend zielführende Bedingungen analytisch hergeleitet werden. Die analytischen Ergebnisse stimmen exzellent mit numerischen Quantendynamiksimulationen überein. Die theoretischen Vorhersagen für das ^{87}Rb Atom wurden inzwischen mit Hilfe der hoch-kontrastreichen Ramsey Interferometrie von experimentellen Partnern in Japan mit einer Genauigkeit von drei Attosekunden bestätigt.

Der zweite Teil untersucht den Elektronenfluss während der Ladungsmigration in orientierten Benzolmolekülen. Dabei werden für zwei unterschiedliche nicht-aromatische elektronische Superpositionszustände verschiedene Typen der adiabatischen Ladungsmigration auf der Attosekundenzeitskala aufgezeigt. Aus der Kenntnis der zeitabhängigen Viel-Elektronen-Wellenfunktion als Linearkombination elektronischer Eigenfunktionen, die mit Hilfe konventioneller Verfahren der Quantenchemie berechnet werden, werden Ausdrücke für die Zeit-Evolution der Ein-Elektronen-Dichte und des Elektronenflusses hergeleitet. Daraus ergibt sich die jeweilige Zahl der Elektronen, die zur Ladungsmigration beitragen, sowie der Mechanismus der Ladungsmigration.

Zusammenfassend zeigt diese Dissertation erstmals, dass die Symmetrie der Elektronenstruktur von Atomen und Molekülen mit Hilfe von einfachen Laserpulsen nicht nur gebrochen, sondern auch wiederhergestellt werden kann. Die Strategien der kohärenten Laserkontrolle verlangen dazu die strenge Kontrolle der zeitabhängigen Phasen der elektronischen Wellenfunktionen. Praktische Anwendungen erfordern dafür eine zeitliche Genauigkeit von wenigen Attosekunden - also noch viel genauer als die ohnehin schon ultrakurze Zeitskala der Ladungsmigration. Untersuchungen der Ladungsmigration zeigen, dass vergleichbar ähnliche Superpositionen elektronischer Wellenfunktionen zu quantitativ verschiedenen Elektronenflusszahlen führen können.

Contents

List of Publications xi

1 Introduction 1

2 Theoretical Background 7
- 2.1 The Time-Dependent Schrödinger Equation[4, 98] . . . 7
  - 2.1.1 The Born-Oppenheimer approximation[4, 98, 100] . . . 8
  - 2.1.2 Analysis of Electron Dynamics . . . 10
- 2.2 The Solution of the Time-Independent Electronic Schrödinger equation[4, 98, 99] . . . 11
  - 2.2.1 The Hartree-Fock Method . . . 11
  - 2.2.2 The Configuration Interaction Method[4, 98, 103] . . . 15

3 Attosecond Control Symmetry Breaking and Restoration 19
- 3.1 Molecular Symmetry[103, 109, 110] . . . 19
- 3.2 Symmetry Breaking and Restoration at the Ground State . . . 20
  - 3.2.1 General Theory for Symmetry Restoration at Ground State . . . 20
  - 3.2.2 Design of Circularly Polarized Pulse . . . 27
  - 3.2.3 Design of Linearly Polarized Pulse . . . 28
  - 3.2.4 Numerical Propagator . . . 29
- 3.3 Extended Theory for Symmetry Restoration at the Excited State . . . 30

4 Publications 35
- Paper SR1 . . . 37
- Paper SR2 . . . 51
- Paper SR3 . . . 79
- Paper SR4 . . . 101
- Paper CM1 . . . 137
- Paper CM2 . . . 149

5 Summary 157

Bibliography 173

List of Publications

Symmetry Breaking and Restoration

Paper SR1 **C. Liu**, J. Manz, K. Ohmori, C. Sommer, N. Takei, J. C. Tremblay, and Yichi Zhang

"Attosecond Control of Restoration of Electronic Structure Symmetry"

Phys. Rev. Lett. **121**, 173201 (2018)

DOI: 10.1103/PhysRevLett.121.173201

Paper SR2 **C. Liu**, J. Manz, and J. C. Tremblay

"From Molecular Symmetry Breaking to Symmetry Restoration by Attosecond Quantum Control"

Progress in Ultrafast Intense Laser Science XIV, Springer, **118**, 117-140 (2018)

DOI: 10.1007/978-3-030-03786-4

Paper SR3 **C. Liu**, J. Manz, and J. C. Tremblay

"From Symmetry Breaking via Charge Migration to Symmetry Restoration in Electronic Ground and Excited States: Quantum Control on the Attosecond Time Scale"

Appl. Sci. **9**, 953 (2019)

DOI: 10.3390/app9050953

Paper SR4 **C. Liu**, J. Manz, and J. C. Tremblay

Comment on "Molecules in confinement in clusters, quantum solvents and matrices: general discussion"

Faraday Discuss. **212**, 569-601 (2018)

DOI: 10.1039/C8FD90053A

Charge Migration

Paper CM1 G. Hermann, **C. Liu**, J. Manz, B. Paulus, J. F. Pérez-Torres, V. Pohl, and J. C. Tremblay

"Multidirectional Angular Electronic Flux during Adiabatic Attosecond Charge Migration

in Excited Benzene"

J. Phys. Chem. A **120**, 5360–5369 (2016)

DOI: 10.1021/acs.jpca.6b01948

Paper CM2 G. Hermann, **C. Liu**, J. Manz, B. Paulus, J. F. Pérez-Torres, V. Pohl, and J. C. Tremblay

"Attosecond Angular Flux of Partial Charges on the Carbon Atoms of Benzene in Non-Aromatic Excited State"

Chem. Phys. Lett. **683**, 553–558 (2017)

DOI: 10.1016/j.cplett.2017.01.030

Chapter 1

Introduction

Symmetry is a fundamental phenomenon in science and plays a central role in describing the laws of physics and chemistry for our understanding of matter. Symmetry breaking is often the origin of innumerable important effects, such as the universe evolution, biological evolution, chemical reactions, Jahn-Teller effects and so on, from elementary particle physics,[1] biology[2] to cosmology[3].

In this dissertation, symmetry is defined in terms of point group symmetry. The characters determine the irreducible representations (IRREPs) for a given symmetry. Symmetry IRREPs are helpful for understanding the energy eigenfunctions and discovering the selection rules for transitions among molecular eigenstates. The symmetries in molecule manifest themselves in the form of the potential energy surface, as well as in the electronic wave functions of the molecule.[4] These symmetries in turn dictate symmetries in the molecular dynamics. Breaking the symmetry of the electronic structure is to redistribute the electronic configuration such that the wave function can no longer be assigned to a single IRREP of the original symmetry point group, and restoring the symmetry is to reshape the wave function such that the IRREPs can be re-assigned into the original symmetry point group.

In most cases, symmetry breaking is irreversible, but there are also some famous exceptions of symmetry generation or restoration. For example, the formation of the Buckminsterfullerene C_{60} with icosahedral symmetry[5] demonstrates that the symmetry can be generated in chemical synthesis. Laser induced high harmonic generation (HHG)[6–10] also denotes a kind of symmetry restoration, in which laser pulses are applied to a highly symmetric ground state. In a first step, the system is ionized by a laser pulse, breaking the symmetry. In a second step, the laser brings the photo-emitted electron back to the ion-core such that it forms a highly asymmetric excited collision pair. In a third step, the system is de-excited back to the high symmetric ground state by spontaneous emission of high harmonics. This can be considered as spontaneous symmetry restoration, although it was never recognized as such. Moreover, the efficiency of symmetry restoration by HHG is quite small e.g. much less than 1%. Here we are aiming at developing a theory to restore the symmetry $> 99.9\%$ coherent controlled by ultrashort laser pulses. The first indication of the possibility of laser control

symmetry breaking and restoration in atoms may be related to some early works on Ramsey fringes in Rydberg atoms by Alber et al[11] and Noordam et al.[12] They showed that after coherently exciting a superposition state, one can de-excite the system back to the ground state by applying a second pulse. Although conceptually similar, no one recognized underlying phenomenon symmetry restoration as such.

In a similar experiment, Arasaki et al[13] excited a wave packet of the excited states of NO_2 molecule (with C_{2v} symmetry in ground state) and let it evolve to a conical intersection. Thus breaking the molecular symmetry from C_{2v} to C_s. After some time, the original symmetry C_{2v} appears again after the wave function missed the conical intersection . This can be considered as symmetry restoration controlled by laser, but it is a transient phenomenon for a very short time dictated by the topology the potential energy surface. We will show in this dissertation another strategy of laser control stationary symmetry breaking and restoration, which is based on a perturbation of the electronic state of the system and can be of much longer durations.

Electronic structure symmetry breaking and restoration can be treated as spatial redistribution of electronic charge in atoms and molecules, which is the most important primary events in all photoinduced processes. The concept of symmetry restoration is intimately related to that of phase retrieval in quantum information technologies.[14] It is already well known that a laser pulse can break the symmetry[8, 11–24] of atoms and molecules by creating a superposition state of ground and excited state, which initiates ultrafast charge migration[20, 25–34] with period from few femtoseconds (fs) down to few hundreds of attoseconds (as), which depends on the energy difference between the electronic ground state and the excited state. Its observation and control in real time represents rather a challenge in coherent control[14, 35–37] for state-of-the-art experimental techniques.

Understanding these dynamics at the atomic level generally requires a time resolution in the attosecond time domain to visualize electronic motion. This accuracy essential not only to obtain fundamental insights into these processes but also, on a longer perspective, for improving the associated applications.[38]

For instance, laser control symmetry restoration of electronic structure is very useful in chemical reactions[39–41] and charge migration processes.[20, 25–34] The recent applications using counterrotating right and left circularly polarized laser pulses open new application perspectives, e.g., switching intramolecular ring currents and induced magnetic fields,[42] the production of electron vortices,[43] selective generation of circularly polarized high harmonics depending on the conformity of the symmetries of the laser field and the molecule,[44–46] and time-dependent monitoring of symmetry breaking.[47] Ultrashort laser pulses is an extremely powerful tool for the investigation, manipulation and control

of ultrafast processes occurring on timescales down to the attosecond regime. Especially, pairs of ultrashort laser pulses have been a matter of particular interest due to their controllable temporal delay and the relative phase shift between the two pulses.[48] By using quantum control calculation one can selectively manipulate the molecules, and by controlling electronic dynamics one can control molecular properties such as the electronic structure symmetry breaking and restoration.

Here, we investigate a new physical phenomenon: coherent control of intra-atomic and intra-molecular symmetry breaking and symmetry restoration. The goal of this dissertation is to show that laser pulse can not only break the symmetry but also can restore the symmetry. For this purpose, a very simple but with highly symmetric ground state is chosen — the oriented benzene molecule, which is also motivated by a recently fundamental work of laser control aromaticity of benzene molecule by Ulusoy and Nest.[49] Further, the ^{87}Rb atom with an isotropic electronic structure in its ground state is also a very good choice for laser control symmetry breaking and restoration, which is motivated by many various fundamental effects for the excitations of Rydberg states that have been discovered.[50–54]

For the purpose of coherent control symmetry breaking and restoration, we develop four strategies. **Paper** SR1 establishes a new theory of coherent control symmetry breaking and restoration by means of two time-delayed circularly ultrashort laser pulses, with applications to the benzene molecule and ^{87}Rb Rydberg atom. Here, we excite the molecule by applying the first circularly polarized pulses from the electronic ground state to a superposition of the ground and an excited state. After creating the superposition state, in general the symmetry of the electronic structure is reduced, thus the symmetry is broken. Then the second identical time-delayed pulse is used to de-excite the superposition back to the ground state for symmetry restoration with the same IRREP. The first pulse pumps some of the amplitude into excited state, while the second pulse either enhances the population of excited state or pumps the previously create amplitude back to the ground state. The time delay between two pulses must be sufficiently long and their durations are short such that the system evolve in quasi-field-free environment at the central time. The time delay between two pulses must be short enough so that the nuclear motion can be neglected within our simulation of 10 fs. Numerical simulations and analytical results are presented for both models, and the feasibility of symmetry restoration is confirmed by a high contrast Ramsey interferometry experiment for ^{87}Rb atom in 3 as attosecond precision.

Paper SR2 presents the second different strategy, in which we apply two time reversed copy of linearly polarized laser pulses and chirp-up, chirp-down pulses to break and restore the symmetry in ground state with phase condition satisfied. For these two scenarios, we achieve the symmetry restoration by repopulating the IRREP. Is it possible to restore the symmetry with a different IRREP?

To answer this question, in **Paper** SR3 we investigate a general way to restore the symmetry in excited state with different $IRREP_e \neq IRREP_g$ but in same symmetry point group. For this method, the two pulses for symmetry breaking and restoration require neither identical as in SR1, nor time-reversed copy as in SR2. The first pulse can be arbitrary, while the sum of these two pulses has to be a π-pulse to completely excite the system from its electronic ground state to a pure excited state. We quantitatively analyze the time evolution of the final population of the excited state and the dependence of the phase difference on time delay. **Paper** SR4 shows a special case of 50% excitation population, which serves as a bridge of **Paper** SR1, SR2 and SR3. For this case, one can either restore the symmetry in ground state with same IRREPs in same point group or in excited state with different a IRREP in same point group, which depends on the time delay. The studies in the **Paper** SR1 - SR4 focus on the analysis of the dependence of the final population of the excited state on the time delay, and the sensitivity of the phase difference to the time delay.

In all our studies of symmetry breaking and restoration, after applying the first ultrashort pulse a superposition is prepared, which initiates the attosecond ultrafast charge migration process between two degenerate superposition states. However, this ultrafast process is not studied quantitatively in **Paper** SR1 - SR4. Charge migration is an ubiquitous phenomenon with profound implications throughout many areas of chemistry, physics, biology and materials science.[38] It arises whenever multiple electronic states are coherently populated and the measurement and controlling of charge migration is a key goal of attosecond science.[38] It is induced by pure electronic dynamics, which is different from charge transfer driven by nuclear motion and much slower than charge migration. Charge migration was first discussed in 1944 in Quantum Chemistry textbook written by Eyring et al[55] and the first experimental observation was made in 1995 by Weinkauf and Schlag et al.[56–59] The phenomenon was studied mostly by Levine and Remacle,[26, 60, 61] Cederbaum and Kuleff et al,[25, 62–67] Corkum and Bandrauk et al,[23, 68, 69] Fujimura and Lin et al[28, 29, 70] but also by other groups.[20, 27, 30, 71–74] With the current development of laser techniques, it is possible to trace the electronic dynamics with attosecond time resolution.[7, 8, 75–83] Recently, the first experimental observation of the attosecond ultrafast charge migration in ionized iodoacetylene[31] took place. Due to its ability of solving fast temporal events down to the attosecond time scale, charge migration attracts continuous interest since decades years.[38]

The charge migration involved in non-aromatic electronic superposition states of benzene molecule was first investigated by Ulusoy and Nest.[49] They prepared two non-aromatic superpositions of the electronic ground and two lowest-lying singlet excited states by using a sequence of laser pulses, which initiate charge migration in attosecond time scale. They indicated that the six delocalized π-

electrons in an oriented benzene molecule[84–90] are either localized on alternating bonds for Kekulé structures[49, 91] or partially on alternating carbon atoms for the other Lewis structure.[49] Furthermore, they estimated that totally 4.2 electrons move around the ring system for Kekulé structures and 1.5 electrons move in the other non-aromatic superposition. They gave a semi-quantitative estimation that the charge migration between two Kekulé structures is a pincer-type motion but without giving any quantitative analysis of the electron flow, for which we will confirm in **Paper** CM1.

The quantitative analysis for benzene molecule was done by Schild and coworkers,[92] in which they indicated that 0.2 electrons move by stimulating the vibrational motion along the Kekulé mode. Whereas this process refers to charge transfer instead of charge migration. Our interest here is: How do the electrons really move during a charge migration process in ref. [49]?

To answer this question, in **Paper** CM1 and CM2 we illustrate two processes of quantum control of adiabatic attosecond charge migration (AACM) for two different non-aromatic superposition states of benzene molecule. In **Paper** CM1, we prepared two Kekulé structures by exciting the molecule from its electronic ground state to the first lowest-lying singlet excited state by means of series of laser pulses. Accordingly, the electron charges circulate in the ring system in attosecond time scale . Since the nuclei are essentially frozen at this time domain, thus the effect of kinetic couplings (also called non-adiabatic coupling) are negligible, e.g. the process is adiabatic attosecond charge migration. For comparison, the theory for diabatic transitions (with much longer than 10 fs time scale) has been developed by Takatsuka and coworkers.[93–96] there are some theoretical works[20, 26, 31, 49, 57] on adiabatic process but not enough for addressing our questions listed above. for determining the direction of the electron motion and the number of electrons that participate in AACM process, we need to analyze the electronic flux and density difference. The adiabatic attosecond charge migration (AACM) is analogous to coherent tunnelling irrespective of different time scales, different meaning of the states and different preparation of the initial state. Therefore, in **Paper** CM1, our goal is to transfer (but not copy) the theory of electronic flux during coherent tunnelling to AACM and develop a new theory of electronic fluxes during AACM in an oriented ring system - benzene molecule. Another task of CM1 is to analyze the angular electronic fluxes quantitatively and determine the direction of electron charge move and further specify the number of electrons that participate in the AACM process. The methods that used here was originally derived for concerted electronic and nuclear fluxes during the coherent tunnelling process, see ref. [97].

In **Paper** CM2, the similar analysis is done for the other non-aromatic superposition state of benzene molecule that was created in ref. [49]. We prepare the superposition by exciting the system from the electronic ground state to the second lowest-lying singlet excited state via series of laser pulses.

Based on the theory and methods that we have developed in **Paper** CM1, we will determine the electronic flux of the partial charges on alternating carbon atoms during AACM and specify the number of electrons that involved in the charge migration. The simulation results indicate that the electron charge flow from the localized alternating carbon atoms to other carbon atoms in pincer-type motion. The studies of **Paper** CM1 and CM2 focus on the quantitative analysis of the electronic dynamics. In a nutshell, this dissertation covers the researches that address the following questions. How to restore the symmetry of electronic structure in atoms and molecules? Which condition should be satisfied for successful symmetry restoration? How do the electron charges really move during the attosecond ultrafast charge migration? How many electrons participate in the charge migration?

The dissertation is organized as follows. The Chapter 2 introduces briefly the basic quantum mechanical theory that will be used for the simulations of this dissertation. The Chapter 3 is the basic theory of coherent control symmetry breaking and restoration that we have developed. The Chapter 4 serves as a list of the academic publications during my doctoral study. At the end, in Chapter 5 I summarize the primary results and propose an outlook based on the present work.

Chapter 2

Theoretical Background

In this chapter, I will give a brief review of some quantum chemistry basic concepts and give a theoretical background, which are necessary for understanding all publications presented in this dissertation.

2.1 The Time-Dependent Schrödinger Equation[4, 98]

We assume that the nuclei and electrons are point masses and neglect spin-orbit and other relativistic interactions. In non-relativistic quantum systems, the time evolution of the molecular wave function is determined by the time-dependent Schrödinger equation,[99] which is written as

$$i\hbar\frac{\partial}{\partial t}|\Phi_{tot}(\mathbf{q},\mathbf{Q},t)\rangle = \left[\hat{H}_{tot}(\mathbf{r},\mathbf{R}) + \hat{V}_{int}(\mathbf{r},\mathbf{R},t)\right]|\Phi_{tot}(\mathbf{q},\mathbf{Q},t)\rangle \tag{2.1}$$

with $\hbar$ and i the reduced Plank constant and the imaginary unit, respectively. The total molecular wave function $\Phi(\mathbf{q},\mathbf{Q},t)$ depends on time t, $4N_e$ electronic coordinates $\mathbf{q} = \{\mathbf{q},\theta\} \equiv \{r_i,\theta_i\}_{i=1}^{N_e}$ with $3N_e$ electronic spatial coordinates r and N_e spin coordinates θ, and $4N_n$ nuclear coordinates $\mathbf{Q} = \{\mathbf{R},\mathbf{\Theta}\} \equiv \{R_\alpha,\Theta_\alpha\}_{\alpha=1}^{N_n}$ with $3N_n$ nuclear spatial coordinates Q and N_n nuclear spin coordinates Θ. $\hat{H}_{tot}(\mathbf{r},\mathbf{R})$ is the time-independent molecular Hamiltonian and $\hat{V}_{int}(\mathbf{r},\mathbf{R},t)$ is the time-dependent interaction operator of the molecular system interacting with an external electric field, which can be defined in the semiclassical dipole approximation as following

$$\hat{V}_{int}(\mathbf{r},\mathbf{R},t) = -\vec{d}(\mathbf{r},\mathbf{R})\cdot\vec{\epsilon}(t) \tag{2.2}$$

Here $\vec{d}(\mathbf{r},\mathbf{R})$ is the molecular dipole operator, and $\vec{\epsilon}(t)$ is the electric field operator.

The total molecular Hamiltonian operator $\hat{H}_{tot}(\mathbf{r},\mathbf{R})$ is written as

$$\begin{aligned}\hat{H}_{tot}(\mathbf{r},\mathbf{R}) &= \sum_i -\frac{\hbar^2}{2m}\nabla_i^2 + \sum_i\sum_{j>i}\frac{e^2}{4\pi\varepsilon_0|\mathbf{r}_i-\mathbf{r}_j|} + \sum_\alpha -\frac{\hbar^2}{2M_\alpha}\nabla_\alpha^2 + \sum_\alpha\sum_{\beta>\alpha}\frac{Z_\alpha Z_\beta e^2}{4\pi\varepsilon_0|\mathbf{R}_\alpha-\mathbf{R}_\beta|} + \sum_\alpha\sum_i -\frac{Z_\alpha e^2}{4\pi\varepsilon_0|\mathbf{r}_i-\mathbf{R}_\alpha|} \\ &= \hat{T}_e(\mathbf{r}) + \hat{V}_e(\mathbf{r}) + \hat{T}_N(\mathbf{R}) + \hat{V}_N(\mathbf{R}) + \hat{V}_{eN}(\mathbf{r},\mathbf{R})\end{aligned} \tag{2.3}$$

where α,β refer to the nuclei and i,j refer to the electrons. $\{\mathbf{r},\nabla_i\}$ refers to the electron coordinates and momenta, $\{\mathbf{R},\nabla_\alpha\}$ refers to the nuclear coordinates and momenta. m,e are the rest mass and charge of the electron, respectively. M_α, Z_α are the mass and the charge of the $\alpha-th$ nuclei. ε_0 is the vacuum permittivity. The first term in (2.3) is the electronic kinetic energy operator. The second term is the interelectronic Coulomb repulsions. The third term is the nuclear kinetic energy operator. The fourth term is the internuclear Coulomb repulsions. The last term is the electron-nuclear attractions. The total molecular Hamiltonian (2.3) is formidable enough to terrify the quantum chemists. Because even for the simplest molecule H_2^+, which consists of three particles, it's impossible to solve its time-independent Schrödinger equation analytically. To overcome this difficulty, we need to make further approximations.

2.1.1 The Born-Oppenheimer approximation[4, 98, 100]

Since the nuclei are much heavier than the electrons, they move much more slowly than the electrons. Thus one can consider that the electrons in a molecule are moving in the mean field of fixed nuclei - the Born-Oppenheimer approximation,[100] which is called the most fundamental approximation in quantum chemistry. Within this approximation, the third term of (2.3) can be neglected and the fourth term of (2.3) can be considered to be a constant. But any constant added to an operator has no effect on the operator eigenfunctions and only adds to the operator eigenvalues. Hence, within the clamped-nuclei approximation, we neglect the fourth term of (2.3), the remaining terms in (2.3) are called the electronic Hamiltonian, which written as:

$$\hat{H}_e(\mathbf{r};\mathbf{R}) = \sum_i -\frac{\hbar^2}{2m}\nabla_i^2 + \sum_i\sum_{j>i}\frac{e^2}{4\pi\varepsilon_0|\mathbf{r}_i-\mathbf{r}_j|} + \sum_\alpha\sum_i -\frac{Z_\alpha e^2}{4\pi\varepsilon_0|\mathbf{r}_i-\mathbf{R}_\alpha|} \tag{2.4}$$

The electronic Hamiltonian $\hat{H}_e(\mathbf{r};\mathbf{R})$ depends parametrically on the nuclear coordinates $\mathbf{R}$. For each fixed nuclear configuration, the time evolution of the electronic eigenfunction can be obtained by solving the time-independent electronic Schrödinger equation

$$\hat{H}_e(\mathbf{r};\mathbf{R})|\Psi_\lambda(\mathbf{r};\mathbf{R})\rangle = E_\lambda(\mathbf{R})|\Psi_\lambda(\mathbf{r};\mathbf{R})\rangle. \tag{2.5}$$

Here $|\Psi_\lambda(\mathbf{r};\mathbf{R})\rangle$ is the stationary electronic wave function, which describes the motion of the electrons and explicitly depends on the electronic coordinates, and also depends parametrically on the nuclear coordinates. $|\Psi_\lambda(\mathbf{r};\mathbf{R})\rangle$ is a different function of the electronic coordinates for different arrangements of nuclei. Different arrangements are adopted and the calculation are repeated, thus we get a set of $E_\lambda(\mathbf{R})$ by solving the eqn. (2.5). This set of the energies describes the motion of nuclei. The function denotes the molecular potential energy surface.

According to the Hermitian property of the electronic Hamiltonian $\hat{H}_e(\mathbf{r};\mathbf{R})$, the orthonormality condition of the

$$\langle\Psi_\lambda|\Psi_\nu\rangle \equiv \int \Psi^*_\lambda(\mathbf{r};\mathbf{R})\Psi_\nu(\mathbf{r};\mathbf{R})d\mathbf{r} = \delta_{\lambda\nu} \tag{2.6}$$

which shows that the Dirac notation of the inner product of two wave functions indicates an integration over all the electronic coordinates $\mathbf{r}$. The electronic wave functions obtained from the solution of eqn. (2.5) form a complete basis set, thus the total molecular wave function can be expanded as a linear combination of these basis functions by using the Born-Huang ansatz [101]

$$|\Phi_{tot}(\mathbf{q},\mathbf{R},t)\rangle = \sum_\lambda |\Psi_\lambda(\mathbf{q};\mathbf{R})\rangle|\chi_\lambda(\mathbf{R},t)\rangle \tag{2.7}$$

with $|\chi_\lambda(\mathbf{R},t)\rangle$, a function of the nuclear coordinates, acting as time-dependent expansion coefficients, referring to the nuclear vibrational wave functions. $|\Psi_\lambda(\mathbf{q};\mathbf{R})\rangle$ is an electronic wave function, which depends parametrically on the nuclear geometry. Inserting this ansatz into the time-dependent Schrödinger equation (2.1) and integrating over the electronic wave functions by multiplying $\langle\Psi_\lambda(\mathbf{q};\mathbf{R})|$ from the left, we get the equation of the motion for the nuclei

$$i\hbar\frac{\partial}{\partial t}|\chi_\lambda(\mathbf{R},t)\rangle = \left[\hat{T}_N(\mathbf{R}) + E_\lambda(\mathbf{R}) + \left(\sum_\nu \Lambda_{\lambda\nu}(\mathbf{R})\right) + \hat{V}_{int}(\mathbf{R},t)\right]|\chi_\lambda(\mathbf{R},t)\rangle \tag{2.8}$$

where the non-adiabatic (or kinetic) coupling term $\Lambda_{\lambda\nu}(\mathbf{R})$ is the dynamical interactions between the electronic and nuclear motion, which can be written as

$$\Lambda_{\lambda\nu}(\mathbf{R}) = -\sum_\alpha^{N_n}\frac{\hbar^2}{2M_\alpha}\left[2\vec{\Lambda}^{(1)}_{\lambda\nu}(\mathbf{R})\cdot\vec{\nabla}_{\vec{R}_\alpha} + \Lambda^{(2)}_{\lambda\nu}(\mathbf{R})\right]. \tag{2.9}$$

Here, the first-order coupling terms $\vec{\Lambda}^{(1)}_{\lambda\nu}(\mathbf{R}) = \langle\Psi_\lambda|\vec{\nabla}_{\vec{R}_\alpha}|\Psi_\nu\rangle$ are vectorial quantities, and the second-order coupling terms $\Lambda^{(2)}_{\lambda\nu}(\mathbf{R}) = \langle\Psi\Psi_\lambda|\nabla^2_{\vec{R}_\alpha}|\Psi_\nu\rangle$ are scalar functions.[4, 102] Neglecting these two non-adiabatic coupling terms, e.g. the uncoupling electronic states for field-free Hamiltonian, leads to the Born-Oppenheimer approximation.[100]

For a system with time-dependent Hamiltonian, the analysis of the electron dynamics can quanti-

tatively reveal the mechanistic details of the internal system.

2.1.2 Analysis of Electron Dynamics

In this dissertation, we will not consider the nuclear vibrational-rotational problem but only focus on the electronic problems for closed shell systems with neglecting the spin coordinates. The electronic Time-Dependent Schrödinger Equation is written as

$$i\hbar\frac{\partial}{\partial t}|\Psi(\mathbf{r},t)\rangle = \left[\sum_i -\frac{\hbar^2}{2m}\nabla_i^2 + \sum_i\sum_{j>i}\frac{e^2}{4\pi\varepsilon_0|\mathbf{r}_i-\mathbf{r}_j|} + \sum_\alpha\sum_i -\frac{Z_\alpha e^2}{4\pi\varepsilon_0|\mathbf{r}_i-\mathbf{R}_\alpha|} + \hat{V}_{int}(\mathbf{r},\mathbf{R},t)\right]|\Psi(\mathbf{r},t)\rangle \tag{2.10}$$

If the Hamiltonian operator does not depend on the time explicitly, the solution is

$$\Psi(\mathbf{r},t) = e^{-i\hat{H}_{tot}t/\hbar}\Psi(\mathbf{r}), \tag{2.11}$$

which represents the evolution of the complex phases associated with the stationary states. The spatial part $\Psi(\mathbf{r})$ satisfies the time-independent Schrödinger equation.

The time- and space-resolved analysis of ultrafast electronic processes are necessary for fully understanding the intrinsic mechanism of electron dynamics in a molecule. In such a case, time-dependent one-electron density

$$\rho(\vec{r},t) = \sum_{\lambda\nu}\int d\mathbf{R}[\chi_\nu^*(\mathbf{R},t)\chi_\nu(\mathbf{R},t)]\rho_{\lambda\nu}(\vec{r};\mathbf{R}) \tag{2.12}$$

is often used for the analysis of correlated electron dynamics. Here $\chi_\lambda(\mathbf{R},t)$ is the nuclear wave function and $\rho_{\lambda\nu}(\vec{r};\mathbf{R})$ is the time-dependent electronic transition density between electronic state λ and ν, written as

$$\rho_{\lambda\nu}(\vec{r};\mathbf{R}) = \int ... \int d\vec{r}_2 ... d\vec{r}_{N_e}\Psi_\lambda(\mathbf{r};\mathbf{R})\Psi_\nu(\mathbf{r};\mathbf{R}) \tag{2.13}$$

The time-derivative of the time-dependent one-electron density refers to as electron flow, and the spatially resolved instantaneous flow of electrons is explained by the time-dependent electronic flux density as follows

$$\vec{j}(\vec{r},t) = \sum_{\lambda\nu}\int d\mathbf{R}[\chi_\nu^*(\mathbf{R},t)\chi_\nu(\mathbf{R},t)]\vec{j}_{\lambda\nu}(\vec{r};\mathbf{R}) \tag{2.14}$$

The time-independent electronic transition flux density from state λ and state ν is

$$\vec{j}(\vec{r};\mathbf{R}) = -\frac{i\hbar}{2m}\int ... \int d\vec{r}_2 ... d\vec{r}_{N_e}(\Psi_\nu(\mathbf{r};\mathbf{R})\nabla_{\vec{r}}\Psi_\lambda(\mathbf{r};\mathbf{R}) - \Psi_\lambda(\mathbf{r};\mathbf{R})\nabla_{\vec{r}}\Psi_\nu(\mathbf{r};\mathbf{R})) \tag{2.15}$$

Within clamped nuclei approximation, diagonal terms correspond to the adiabatic electronic flux den-

sity and is zero when the electronic states are real-valued. The relation between the time-dependent electron density $\rho(\vec{r},t)$ and the electronic flux density $\vec{j}(\vec{r},t)$ is called the electronic continuity equation[99]

$$\frac{\partial}{\partial t}\rho(\vec{r},t) + \nabla_{\vec{r}} \cdot \vec{j}(\vec{r},t)) = 0. \tag{2.16}$$

The integration of the time-derivation of the electron density for a certain time interval $[t_0, t]$ from a given initial condition is called the density difference, taking the following form

$$\Delta\rho(\vec{r},t) = \int_{t_0}^{t} \frac{\partial\rho(\vec{r},t')}{\partial t'} = \rho(\vec{r},t) - \rho(\vec{r},t_0), \tag{2.17}$$

which is often used to analyse the charge migration process. Furthermore, the integration of the density difference gives the number of electrons that flow

$$y = \int \Delta\rho(\vec{r},t)dt \tag{2.18}$$

The accuracy depends on the wave function. The following section will focus on the methods to get an acceptable wave function.

2.2 The Solution of the Time-Independent Electronic Schrödinger equation [4, 98, 99]

From eqn. (2.5) we can get the molecular equilibrium geometry and vibrational frequencies, and the electronic wave function contains lots of useful information about molecular properties such as dipole moments, polarizability, etc. That's the reason why we want to solve the electronic Schrödinger equation. The solution of the Schrödinger equation is still so complicated even after making the Born-Oppenheimer approximation (even for H_2^+). Therefore, further approximations must be applied.

2.2.1 The Hartree-Fock Method

Central to the solution of such problems is the Hartree-Fock approximation, in which the electron-electron repulsion is treated in the average field $\hat{v}_{eff}(\mathbf{r}_i;\mathbf{R})$ - Hartree-Fock potential, which due to the presence of the other electrons. If the one-electron Hamiltonian can include the effects of electron-electron repulsion in an average way, the N_e-electron Hamiltonian is a sum of N_e one-electron Hamil-

tonians. Within this mean-field method, the overall electronic Hamiltonian can be written as

$$\hat{H}_e(\mathbf{r};\mathbf{R}) = \sum_i^{N_e} \left(-\frac{\hbar^2}{2m_e}\nabla_i^2 + \hat{v}_{eff}(\mathbf{r}_i;\mathbf{R}) \right) + \hat{V}_N(\mathbf{R}), \tag{2.19}$$

where the internuclei repulsion $\hat{V}_N(\mathbf{R})$ is a constant factor, electrons are all indistinguishable. So the time-independent electronic Schrödinger equation can be reduced from a N_e-electron problem to N_e coupled one-electron problems. The overall wave function is built from products of one-electron wave functions (Hartree Product).

$$\Psi^{HP}(\mathbf{q}_1, \mathbf{q}_2, ..., \mathbf{q}_{N_e};\mathbf{R}) = \psi_1(\mathbf{q}_1;\mathbf{R})\psi_2(\mathbf{q}_2;\mathbf{R})\cdots\psi_{N_e}(\mathbf{q}_{N_e};\mathbf{R}) \tag{2.20}$$

Each one-electron wave function $\psi_a(\mathbf{q}_i;\mathbf{R})$, corresponding to an orthonormal spin orbital a occupied by an electron i, can be defined as the product of a spatial orbital $\phi_a(\mathbf{r}_i;\mathbf{R})$ and a spin function $\sigma(\theta_i)$.

$$\psi_a(\mathbf{q}_i;\mathbf{R}) = \phi_a(\mathbf{r}_i;\mathbf{R})\sigma(\theta_i) \tag{2.21}$$

$\sigma(\theta_i)$ is either a spin up or a spin down function for fermions. For a many-electron problem, the wave function must be antisymmetric with respect to the interchange of the coordinate $\mathbf{q}$ of any two electrons, which is called the Pauli exclusion principle or antisymmetry principle.

$$\Psi(\mathbf{q}_1, ..., \mathbf{q}_i, ..., \mathbf{q}_j, ..., \mathbf{q}_{N_e};\mathbf{R}) = -\Psi(\mathbf{q}_1, ..., \mathbf{q}_j, ..., \mathbf{q}_i, ..., \mathbf{q}_{N_e};\mathbf{R}). \tag{2.22}$$

But a basic deficienty in the Hartree Product is that it takes no account of the indistinguishability of electrons, but distinguishes each electron a specific spin orbital. So that the Hartree Product does not satisfy the antisymmetry principle.

For making up this disadvantage, it comes up an approach to make N_e electrons occupying N_e spin orbitals without specifying the which electron is in which orbital, which is known as Slater determinant. For a N_e-electron system, the generalization of the antisymmetric wave function can be written as a Slater determinant

$$\Psi_{SD}(\mathbf{q}_i;\mathbf{R}) = \frac{1}{\sqrt{N_e!}} \begin{vmatrix} \psi_a(\mathbf{q}_1;\mathbf{R}) & \psi_a(\mathbf{q}_2;\mathbf{R}) & \cdots & \psi_a(\mathbf{q}_{N_e};\mathbf{R}) \\ \psi_b(\mathbf{q}_1;\mathbf{R}) & \psi_b(\mathbf{q}_2;\mathbf{R}) & \cdots & \psi_b(\mathbf{q}_{N_e};\mathbf{R}) \\ \vdots & \vdots & \ddots & \vdots \\ \psi_{N_e}(\mathbf{q}_1;\mathbf{R}) & \psi_{N_e}(\mathbf{q}_2;\mathbf{R}) & \cdots & \psi_{N_e}(\mathbf{q}_{N_e};\mathbf{R}) \end{vmatrix} \equiv |\psi_a\psi_b\cdots\psi_{N_e}\rangle \tag{2.23}$$

Here, $\frac{1}{\sqrt{N_e!}}$ is the normalization factor. $\psi_a(\mathbf{q}_i;\mathbf{R})$ is the a^{th} spin orbital occupied by electron i with its spatial molecular orbital (MO) and spin function $\mathbf{q}_i \equiv \{\mathbf{r}_i, \theta_i\}$. We can see that the sign of the determinant changes when we interchange the coordinates of any of two electrons by interchanging two corresponding rows of the determinant, which means that the Slater determinant meet the requirement of the antisymmetry principle. A N_e electron closed shell system contains $N_e/2$ spin orbitals with spin-up function and $N_e/2$ spin orbitals with spin-down function, which leads a spin-free representation of the wave function when we integrate over all N_e spin orbitals. The Slater determinant is invariant for any linear transformation of the occupied spatial orbitals.

Within the Hartree-Fock approximation, a single Slater determinant is used to model the total electronic wave function of the ground state in the time-independent electronic Schrödinger equation (2.5). By minimizing the energy with respect to the choice of the spin orbitals in the Slater determinant wave function (2.23), we can obtain a set of effective one-electron eigenvalue equations, the Hartree-Fock equations. For a closed shell system, the spin part of wave function can be integrate out to get a spin-free representation of the wave function. The Hartree-Fock equation for closed shell system can be derived as following

$$\hat{f}(\mathbf{r}_i;\mathbf{R})\psi_a(\mathbf{r}_i;\mathbf{R}) = E_a(\mathbf{R})\psi_a(\mathbf{r}_i;\mathbf{R}) \tag{2.24}$$

$E_a(\mathbf{R})$ is the orbital energy of the a^{th} spin orbital; $\hat{f}(\mathbf{r}_i;\mathbf{R})$ is the Fock operator, which refers to the effective Hamiltonian of the one-electron eigenvalue equation

$$\hat{f}(\mathbf{r}_i;\mathbf{R}) = -\frac{\hbar^2}{2m_e}\nabla^2_{\mathbf{r_i}} - \sum_i^{N_e}\sum_\alpha^{N_n}\frac{Z_\alpha e^2}{4\pi\varepsilon_0|\mathbf{r_i}-\mathbf{R_{ff}}|} + \hat{v}_{eff}(\mathbf{r}_i;\mathbf{R}). \tag{2.25}$$

The effective potential consists of the classical Coulomb potential energy operator $\hat{J}_b(\mathbf{r}_i;\mathbf{R})$ and non-classical exchange potential energy operator $\hat{K}_b(\mathbf{r}_i;\mathbf{R})$

$$\hat{v}_{eff}(\mathbf{r}_i;\mathbf{R}) = \sum_b^{N_e}\left[\hat{J}_b(\mathbf{r}_i;\mathbf{R}) - \hat{K}_b(\mathbf{r}_i;\mathbf{R})\right]. \tag{2.26}$$

In this expression, the sum is over all spin orbitals. The Coulomb operator $\hat{J}_b(\mathbf{r}_i;\mathbf{R})$ and exchange operator $\hat{K}_b(\mathbf{r}_i;\mathbf{R})$ are defined as follows:

$$\begin{aligned}\hat{J}_b(\mathbf{r}_i;\mathbf{R}) &= \int \psi_b^*(\mathbf{r}_i;\mathbf{R})\frac{e^2}{4\pi\varepsilon_0|\mathbf{r}_i-\mathbf{r}_j|}\psi_b(\mathbf{r}_i;\mathbf{R})d\mathbf{r}_i \\ \hat{K}_b(\mathbf{r}_i;\mathbf{R}) &= \int \psi_b^*(\mathbf{r}_i;\mathbf{R})\frac{e^2}{4\pi\varepsilon_0|\mathbf{r}_i-\mathbf{r}_j|}\psi_a(\mathbf{r}_i;\mathbf{R})d\mathbf{r}_i.\end{aligned} \tag{2.27}$$

The Coulomb and exchange operators are defined in terms of spin orbitals rather than in terms of spatial wave functions. By solving the eqn. (2.24) with corresponding Fock operator $\hat{f}(\mathbf{r}_i;\mathbf{R})$, we can get all the spin orbitals. However, $\hat{f}(\mathbf{r}_i;\mathbf{R})$ depends on the $(n-1)$ occupied spin orbitals, thus one has to make a trial set of spin orbitals to formulate the Fock operator; Then solve the Hartree-Fock equations (2.24) to get a new set of spin orbitals and feedback to optimize the Fock operator, and so on. The reformulation is repeated until a convergence criterion is satisfied and one get a self-consistent solution. This self-consistent procedure is named as Self-Consistent Field (SCF).

At the point, it is clear that the Hartree-Fock SCF procedure is available for atomic numerical calculations, but no feasible procedures for obtaining molecular numerical solutions, thus the improvement measures have to be done. For such a purpose, Roothaan and Hall independently gave a suggestion to expand the spatial part of the spin orbitals as a linear combination of a set of basis functions, which is well known as Molecular Orbitals as Linear Combination of Atomic Orbitals ansatz (MO-LCAO).

$$\psi_a(\mathbf{r}_i;\mathbf{R}) = \sum_{\alpha}^{N_n} \sum_{i_\alpha}^{n_{AO}(\alpha)} C_{i\alpha}^{(a)} \phi_{i_\alpha}(\mathbf{r}_i - \mathbf{R}_\alpha) \tag{2.28}$$

where $C_{i\alpha}^{(a)}$ is the $(i_\alpha)^{th}$ molecular coefficient of MO a, and $\phi_{i_\alpha}(\mathbf{r}_i - \mathbf{r}_\alpha)$ denotes the $n_{AO}^{(\alpha)}$ atomic orbitals centered at atom α.

It is important to choose a proper basis set to get a reasonably accurate AOs, especially for the ground state MO. But the computational cost increases sharply with the basis set getting larger, so AOs have to be justified chosen. The application of the MO-LCAO ansatz leads to the Hartree-Fock-Roothaan-Hall matrix eigenvalue equation

$$\mathbf{FC} = \mathbf{SC}\epsilon \tag{2.29}$$

with the Fock matrix in the AO basis $F_{kk'} = \langle \phi_k | \hat{F}(\mathbf{r}_i;\mathbf{R}) | \phi_{k'} \rangle$, the MO coefficient matrix $\mathbf{C}$, the overlap matrix of the basis function $\mathbf{S}$, and the diagonal MO energy matrix ϵ. One can not solve the equation directly, because the the matrix $\mathbf{F}$ involves Coulomb and exchange integrals which also depend on the spatial wave functions. Therefore, again we must adopt a SCF approach, obtaining with each iteration a new set of coefficients $\mathbf{C}$ and repeating until a convergence criterion is reached.

One can get as many MOs as MO basis functions, but only N_e lowest spin orbitals, which are referred to as the occupied spin orbitals, contribute to the total molecular energy. All other remaining unoccupied orbitals are called virtual spin orbitals.

2.2.2 The Configuration Interaction Method [4, 98, 103]

Hartree-Fock approximation is quantitatively successful in most cases, but still has its limitations. For example, the restricted Hartree-Fock method cannot describe the dissociation correctly; unrestricted Hartree-fock method can give a qualitatively correct description on dissociations but fails to give an accurate potential energy surface. It ignores the electron correlation, e.g. it considers neither the instantaneous electrostatic interactions between electrons, nor the quantum mechanical effects on electron distributions. So that the energy of Hartree-Fock calculation is always larger than the lowest possible ground state energy in a given basis set. The energy difference between the exact energy and the Hartree-Fock energy is the correlation energy, which is negative. In order to obtain the correlation energy to improve the results, many post-Hartree-Fock methods have been developed to approach the exact energy limit. Of all post-Hartree-Fock method, the Configuration Interaction (CI) method is conceptually the simplest one, in which the exact wave functions of the electronic ground and excited states can be expressed as a linear combination of all possible N_e-electron Slater determinants arising from a complete set of spin orbitals by using the linear variational method. One can use these MOs to form Configuration State Functions (CSFs), then the molecular wave function can be written as a linear combination of the CSFs. Each CSF is a linear combination of Slater determinants and an eigenfunction of the spin angular momentum operator with molecular spatial symmetry. Therefore, we can write the exact electronic wave function for any state of the system in the form

$$|\Psi_{CI}\rangle = D_0|\Psi_{HF}^{(0)}\rangle + \left(\frac{1}{1!}\right)\sum_{ar} D_a^r|\Psi_{HF}^{(0)}\rangle_a^r + \left(\frac{1}{2!}\right)^2\sum_{abrs} D_{ab}^{rs}|\Psi_{HF}^{(0)}\rangle_{ab}^{rs} + \cdots \tag{2.30}$$

where $|\Psi_{HF}^{(0)}\rangle$ is the determinant formed from the N_e lowest energy spin orbitals, and the $n-$tuply excited Slater determinants $|\Psi_{HF}^{(0)}\rangle_{ab}^{rs}$... can be constructed from the Hartree-Fock reference wave function. The CI coefficients D_a^r, D_{ab}^{rs}, ... can be optimized by applying the variational principle. A singly excited determinant D_a^r refers to excite a single electron from occupied spin orbital Ψ_a to a virtual spin orbital Ψ_r; a doubly excited determinant D_{ab}^{rs} denotes to excite one electron from Ψ_a to Ψ_r and one from Ψ_b to Ψ_s by imposing specific spin, likewise for other excited determinants. The energy associated with the exact wave function of the ground state in the form (2.30) is the exact non-relativistic ground state energy within the Born-Oppenheimer approximation. In a molecular full CI calculation, one begins with a set of AO basis functions, does a SCF HF calculation to find a set of SCF occupied and virtual MOs. A full CI calculation includes all CSFs of the appropriate symmetry, which are used for a given finite basis set. But the number of determinants increases factorially with the number of electrons and basis functions, such that the computational expense for this exact ansatz is

only affordable for very small systems. Therefore, for most cases, the expansion in eqn. (2.30) must be truncated by considering which types of configurations make significant contributions to $|\Psi_{CI}\rangle$. One truncation scheme is to take a certain excitation levels into account, such as including the singly (S) and doubly (D) excited configuration functions (CISD), or only includes the singly excitations (CIS). The other truncated CI method is Restricted-Active-Space Configuration Interaction (RASCI), where the the electronic wave functions of ground and excited states are obtained as the CI expansion over a restricted set of Slater determinants.[104, 105] However, an important problem of truncated CI methods is their size-inconsistency, which means the energy of two infinitely separated particles is not the sum of the energies of the single particles. Also truncated CI expansions are not size-extensive, which means that the calculated energies scale not properly with the number of particles, so the methods are restricted to small molecules.

As an attractive, Multi-Configurational Self Consistent Field (MCSCF) methods have been developed and widely used in many fields of the molecular sciences. The central idea of MCSCF method is to obtain the electronic wave function with the lowest possible energy by reducing the required configurations and optimizing all the molecular orbitals [106]. MCSCF methods generate accurate wave functions for chemical problems of strong non-dynamical correlation energy, such as bond breaking and dissociations, conical intersections, symmetry breaking problems, spectroscopy and so on. MCSCF wave functions are often used as reference wave function for subsequent multi-reference configuration interaction to include the dynamical correlation.[107] Because it can describe the static electron correlation by including the nearly degenerate electron configurations in the wave function and can get qualitatively correct reference states of molecules by optimizing orbitals and CI coefficients simultaneously. MCSCF method can be considered as the combination of CI and HF, whereas since this combination increases the complexity of the wave function, one usually applies restrictions to both sets of parameters, e.g. core orbitals may be kept fixed and only a small subset of orbitals are selected as an active space, in which all possible configurations are considered.

Complete Active Space SCF method (CASSCF) is the most commonly used MCSCF approach because the wave function can be completely defined by selecting the active orbitals.[107] In CASSCF calculation, the spin orbitals are divided into inactive orbitals, virtual orbitals and active orbitals. All possible configurations constructed from this set of active orbitals with correct space and spin symmetry form a configuration space, where a full configuration interaction (FCI) wave function is generated, and at the same time the orbitals are optimized via relaxing the orbitals and CI coefficients among the selected spaces. The wave function of CASSCF can be expanded as a linear combination

in terms of all CSF with expansion coefficients

$$|\Psi_{CASSCF}\rangle = D_0|\Psi_{HF}^{(k)}\rangle + \left(\frac{1}{1!}\right)\sum_{ar} D_a^r|\Psi_{HF}^{(k)}\rangle_a^r + \left(\frac{1}{2!}\right)^2\sum_{abrs} D_{ab}^{rs}|\Psi_{HF}^{(k)}\rangle_{ab}^{rs} + \cdots \tag{2.31}$$

$|\Psi_{HF}^{(k)}\rangle$ is a Hartree-Fock SCF reference configuration. In order to increase the accuracy of the wave function, one usually increases the number of configurations or the size of active space, but the number of CSFs rises factorially with respect of the number of the electrons and orbitals in the active space, and so does the computational cost. The current limitation of conventional CASSCF implementations is 16 electrons in 16 orbitals. As we see, CASSCF is constructed from a limited set of electronic configurations, therefore does not cover most instantaneous electron-electron interactions, so called dynamic electron correlation. There are some cases we have to include dynamical correlation, such as the negative ions are bound only when a large fraction of the dynamical correlation is taken into account and the shape of some excited states of molecules depend strongly on dynamic correlation effects.[108]

One such scheme is Restricted Active Space SCF method (RASSCF), where the active orbitals are divided into three subsets, each including a different constraint on the number of electrons. Another scheme for covering dynamic electron correlation is Multi-Reference Configuration Interaction (MRCI), where all singly, doubly, ... excited determinants are included. In MRCI calculation, selected CSFs from CASSCF wave function as reference configurations and then CASSCF calculation is restricted to include only the static correlation effects to determine the orbitals. MCSCF wave functions are often used as reference states and excited determinants are formed from a set of reference configurations for use in CI calculation. Then CI is reformed to optimize all coefficients of the included determinants. The reference determinants are singly and doubly excited determinants with respect to the HF SCF wave function, and include single and double excitations from the reference determinants. Therefore the final MRCI calculation will include some triply and quadruply determinants excited from HF SCF wave functions. Due to this, MRCI can cover a large fraction of the exact correlation energy with a much smaller number of determinants, such that MRCI can significantly reduce the size-inconsistency. For balancing the computational cost and accuracy, MRCI is widely used to explore potential energy surfaces, non-adiabatic effects, conical intersections and so on.

Chapter 3

Attosecond Control Symmetry Breaking and Restoration

This chapter is divided into three sections. In Section 3.1, I first give a brief introduce molecular symmetry to demonstrate what is the symmetry of molecule and how to determine the molecular symmetry. Section 3.2 introduces the basic theory of ultrafast attosecond laser control symmetry breaking and restoration in the ground state. Section 3.3 describes the extended theory for breaking the electronic structure symmetry of atoms and molecules electronic ground states and restoring the symmetry in the excited state. All derivations in this chapter are preformed within the Born-Oppenheimer approximation framework.

3.1 Molecular Symmetry[103, 109, 110]

The molecular symmetry has an important effect on physical properties and chemical processes.[111] It can be used to predict or explain a molecule's properties, such as dipole moment, polarizability and its allowed spectroscopic transitions. The molecular symmetry for different electronic states are classified by the Irreducible Representations (IRREPs), which is the simplest representation of the characters of different symmetry operations. In this dissertation, symmetry is defined as symmetry point group, which is a set of all symmetry operations of a molecule. Breaking the symmetry is to distort the electronic wave function such that the IRREPs of the wave function can not be assigned to the initial symmetry point group; and restoring the symmetry is to reshape the electronic wave function such that the IRREPs of the wave function can be reassigned into the original symmetry point group, irrespective of any changes of IRREPs. In a point group, molecular symmetry is described by five types of symmetry element: symmetry axis, plane of symmetry, center of symmetry, rotation-reflection axis, identity. Each symmetry element corresponds to a symmetry operation, which carries a molecule into an equivalent configuration that physically indistinguishable from the original configuration.

E The identity operation.

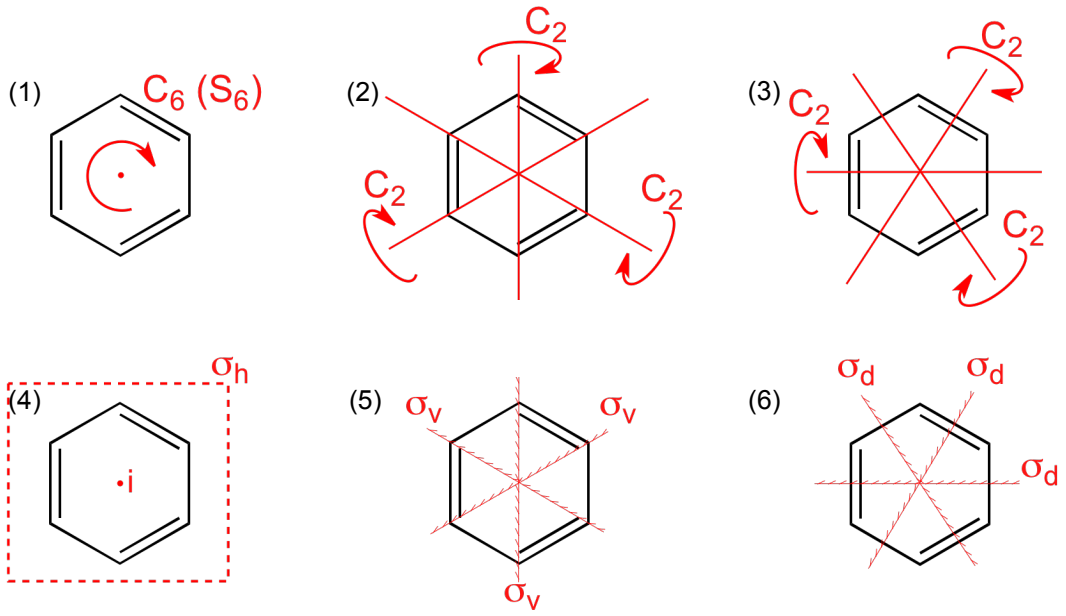

Figure 3.1: All symmetry operations associated with symmetry elements for benzene molecule. There are seven symmetry axis with one C_6 axes and six C_2 axis, and seven symmetry planes with one molecular plane and six planes perpendicular to the molecular plane. (1) shows the operations of C_6 axis with a red arrow; the improper operation of S_6 is carried out by two steps: first a proper rotation by $360/6$ degrees through C_6 axis and then a reflection in a plane that is perpendicular to the C_6 axis. (2) and (3) show six symmetry operations of the symmetry planes C_2, which take place by rotating $360/2$ degrees through associated six symmetry axis C_2. (4) shows the symmetry operations i and σ_h. The inversion operation through the center of the symmetry corresponds to the inversion element i and the reflection operation associated with the horizontal mirror plane σ_h that perpendicular to the symmetry axis C_6 in (1). (5) shows the three reflection symmetry operations of three vertical mirror planes σ_v that includes the symmetry axis C_2 in (2). (6) shows the three reflection symmetry operations of the mirror planes σ_d that includes the symmetry axis C_2 in (3).

C_n An $n-$fold rotation operation, corresponds to a rotation by $2\pi/n$ around a symmetry axis.

σ A reflection operation.

i An inversion operation through a center of symmetry.

S_n An $n-$fold improper rotation operation about an axis of improper rotation.

There are few rules for such a group:

1) The product of any two elements or the square of each element must be an element in the group.

2) One element in the group much commute with all others and leave them unchanged.

3) The associative law of multiplication much hold.

4) Every element must have a reciprocal, which is also an element of the group.

The characters associated with specific operations determine the IRREPs for a given symmetry. The symmetry operations and associated symmetry elements diagram of benzene molecule is shown in Fig. 3.1.

3.2 Symmetry Breaking and Restoration at the Ground State

In this Section, I introduce the general theory of ultrafast attosecond laser control electronic structure symmetry breaking and restoration at the ground state by using circularly polarized pulses and linearly polarized pulses. There are four Subsections in this Section. Subsection 3.2.1 introduces the general theory and derivative of laser control symmetry restoration. Subsection 3.2.2 describes how to design the circularly polarized pulses to control the electronic structure symmetry. Subsection 3.2.3 shows the design of the linearly polarized pulses for the purpose of symmetry restoration in the electronic ground state. Subsection 3.2.4 denotes a strictly unitary numerical propagator that we used for the attosecond precise simulation of ultrafast laser control symmetry breaking and restoration. All work presented here is based on Born-Oppenheimer approximation, in which nuclear motion is neglected.

3.2.1 General Theory for Symmetry Restoration at Ground State

With the molecule interaction with laser fields, the Time Dependent Schrödinger Equation (TDSE) is written as

$$i\hbar\frac{\partial}{\partial t}|\Psi(t)\rangle = H(t)|\Psi(t)\rangle \tag{3.1}$$

where

$$H(t) = H_e - \vec{d}\cdot\vec{\epsilon}(t) \tag{3.2}$$

with the scalar product $\vec{d}\cdot\vec{\epsilon}(t)$ represents the semiclassical interaction of the electronic dipole moment operator $\vec{d}$ and the electric field operator $\vec{\epsilon}(t)$.

The laser driven electronic quantum dynamics of the system is described by the time-dependent wave function $|\Psi(t)\rangle$, which can be expanded as a linear combination of the eigenstates of the stationary Hamiltonian at a chosen level of theory (see **Chapter** 2).

$$|\Psi(t)\rangle = \sum_k c_k(t)|\Psi_k\rangle \tag{3.3}$$

where the sum over k includes a finite set of eigenstates $|\Psi_k\rangle$ with different IRREPs, and $c_k(t)$ are the coefficients. The electronic eigenstates $|\Psi_k\rangle$ and their eigenvalues E_k are obtained as the solutions of the Time-Independent Schrödinger Equation (TISE), which reads

$$H_e|\Psi_k\rangle = E_k|\Psi_k\rangle. \tag{3.4}$$

The labels k denote quantum numbers, or sets of quantum numbers, including the IRREPs. Specifically for a two-level system, we define $k = g$ and $k = e$ denoting the electronic ground state and the target excited state. For molecules, the electronic Hamiltonian H_e accounts for the electronic kinetic energies and intramolecular Coulomb interactions with all particles including electrons and fixed nuclei.

The ansatz (3.3) allows to rewrite the TDSE in matrix form

$$i\hbar\frac{\partial}{\partial t}\mathbf{c}(t) = H(t)\mathbf{c}(t) \tag{3.5}$$

with vector $\mathbf{c}(t)$ denoting the column vector of the coefficients $c_k(t)$. Accordingly, the vector $\mathbf{c}(t) = \big(c_g(t), c_e(t)\big)^{-1}$, with initial condition $\mathbf{c}(t_i) = (1,0)^{-1}$. The Hamiltonian matrix elements are obtained by

$$H_{kl}(t) = \langle\Psi_k|H(t)|\Psi_l\rangle = E_k\delta_{kl} - \vec{d}_{kl}\cdot\vec{\epsilon}(t). \tag{3.6}$$

Here δ_{kl} denotes the Kronecker symbol, and $\vec{d}_{kl} = \langle\Psi_k|\vec{d}|\Psi_l\rangle$ is the $k \to l$ transition dipole matrix element. For symmetry reasons, the diagonal elements vanish, $\vec{d}_{kk} = 0$. Using the two-state approximation with transition dipole matrix elements in eqn. (3.6) for selective excitation from the ground state $|\Psi_g\rangle$ to the target state $|\Psi_e\rangle$ with different IRREPs, we obtain the specific form of the 2×2 Hamilton matrix,

$$H(t) = \begin{pmatrix} H_{gg} & H_{ge}(t) \\ H_{eg}(t) & H_{ee} \end{pmatrix} = \begin{pmatrix} E_g & V(t) \\ V^*(t) & E_e \end{pmatrix} \tag{3.7}$$

with laser-molecule interaction term

$$V(t) = -\frac{1}{\sqrt{2}}d\cdot\left[\epsilon_b s_b(t)\cdot e^{i\omega_c(t-t_b)} + \epsilon_r s_r(t)\cdot e^{i\omega_c(t-t_r)}\right] \tag{3.8}$$

where the d is the transition dipole moment, ϵ_b is the electric field amplitude of the first laser pulse for symmetry breaking, $s_b(t)$ is the electric field envelope, ω_c is the carrier frequency, t_b is the center of the first laser pulse. $\epsilon_r, s_b(t), \omega_c, t_r$ are the corresponding variables of the second laser pulse for symmetry restoration. The first term of eqn. (3.8) serves to break the electronic structure symmetry and the second term to restore the symmetry. The details of design the electric fields will be shown later on in Subsection 3.2.2 and 3.2.3.

The system evolving from the electronic ground state at initial time t_i to a superposition state at

central time t_c, the coefficients at t_c can be obtained by the following formal solution

$$\begin{aligned} \mathbf{c}(t_c = 0) &= \mathbf{U}(t_c, t_i)\mathbf{c}(t_i) \\ &= \hat{T} e^{-i \int_{t_i}^{0} dt' H(t')/\hbar} \mathbf{c}(t_i) \end{aligned} \tag{3.9}$$

where $\mathbf{U}(t_c, t_i)$ is the unitary matrix representation of the time evolution operator, $\hat{T}$ is the time ordering operator. The complex conjugate of eqn. (3.9) is

$$\begin{aligned} \mathbf{c}^*(0) &= \hat{T} e^{i \int_{t_i}^{0} dt' H^*(t')/\hbar} \mathbf{c}(t_i) \\ &= \hat{T} e^{i \int_{t_i}^{0} dt' H(-t')/\hbar} \mathbf{c}(t_i) \\ &= e^{-2i\eta} \mathbf{c}(0), \end{aligned} \tag{3.10}$$

thus the coefficients at central time $t_c = 0$ are real-valued with an irrelevant global phase factor $e^{-2i\eta}$. As one of the conditions for successful symmetry restoration, the Hamiltonian is required to be adjunct upon time reversal

$$\mathbf{H}(t) = \mathbf{H}^*(-t) \tag{3.11}$$

Then we invert eqn.(3.9) and get:

$$\begin{aligned} \mathbf{c}(t_i) &= \mathbf{U}^{-1}(t_c, t_i)\mathbf{c}(t_c = 0) \\ &= \hat{T} e^{-i \int_{0}^{-t_i} dt' H(t')/\hbar} \mathbf{c}^*(0) \\ &= e^{-2i\eta} \hat{T} e^{-i \int_{0}^{t_f} dt' H(t')/\hbar} \mathbf{c}(0) \\ &= e^{-2i\eta} \mathbf{U}(t_f, t_c)\mathbf{c}(t_c = 0) \\ &= e^{-2i\eta} \mathbf{c}(t_f) \end{aligned} \tag{3.12}$$

This denotes that the wave functions at final time t_f and at initial time t_i are the same, so that the associated electronic structure symmetries at t_i and t_f are also the same, irrespective of an irrelevant phase factor $e^{-2i\eta}$. Therefore, we say that the first laser pulse breaks the electronic structure symmetry by exciting the system from its electronic ground state to a superposition state, and the second laser pulse is applied with a proper time delay to stop the charge migration and restore the symmetry via de-exciting the system from the superposition state back to its electronic ground state.

We can obtain the coefficients at an arbitrary time t by solving the TDSE (3.1) analytically[112]

$$\begin{aligned} c_g(t) &= \cos\left\{d\left[\epsilon_b\int_{t_i}^{t}dt' s_b(t') + \epsilon_r\int_{t_i}^{t}dt' s_r(t')\right]/\sqrt{2}\hbar\right\}, \\ c_e(t) &= i\sin\left\{d\left[\epsilon_b\int_{t_i}^{t}dt' s_b(t') + \epsilon_r\int_{t_i}^{t}dt' s_r(t')\right]/\sqrt{2}\hbar\right\}e^{-i\Delta E(t-t_b)/\hbar} \\ &= i\sin\left\{d\left[\epsilon_b\int_{t_i}^{t}dt' s_b(t') + \epsilon_r\int_{t_i}^{t}dt' s_r(t')\right]/\sqrt{2}\hbar\right\}e^{-i\Delta E(t-t_b)/\hbar}. \end{aligned} \tag{3.13}$$

Here we set the electric field is a Gaussian shape function, therefore, by making use of the Gaussian integration $\int_{-\infty}^{+\infty}e^{ax^2}dx = \sqrt{\frac{\pi}{a}}$ and setting $\alpha = \sqrt{\pi}d\epsilon_b\tau_b/\hbar$, the coefficients at t_c can be determined as

$$\begin{aligned} c_g(t_c) &= \cos\left[\frac{1}{\sqrt{2}}d\epsilon_b\int_{t_i}^{t_c}dt' s_b(t')/\hbar\right] = \cos\alpha, \\ c_e(t_c) &= i\sin\left[\frac{1}{\sqrt{2}}d\epsilon_b\int_{t_i}^{t_c}dt' s_b(t')/\hbar\right]e^{-i\Delta E(t_c-t_b)/\hbar} \\ &= \sin\alpha\cdot e^{-i\Delta E(t_c-t_b)/\hbar+i\pi/2} \\ &= \sin\alpha\cdot e^{-i\pi t_d/T+i\pi/2} \\ &= \sin\alpha\cdot e^{i\Delta\eta(t_c)} \end{aligned} \tag{3.14}$$

Here the central time $t_c = (t_b + t_r)/2$, time delay between two laser pulses $t_d = t_r - t_b$, T is the charge migration period, which depends on the energy gap between the ground and excited state, thus determined by

$$T = \frac{h}{E_e - E_g} = \frac{h}{\Delta E} \tag{3.15}$$

For symmetry restoration at the ground state, the second pulse $\vec{\epsilon}_r(t)$ has to have the same polarization as the first pulse $\vec{\epsilon}_b(t)$ with a phase factor to make a zero net effect on the system. Therefore, $\cos[\omega_c(t_b - t_r)] = -1$, from which we obtain the time delay between the two laser pulses

$$t_d = t_r - t_b = (N + 1/2)T, N = 1, 2, 3... \tag{3.16}$$

for our case in **Paper** SR1 $N = 8$ for benzene molecule. Inserting eqn. (3.16) into eqn. (3.14) yields the phase difference between two components of the wave function at the central time t_c

$$\Delta\eta(t_c) = -\pi t_d/T + \pi/2 = -N\pi \text{ modulo } 2\pi \begin{cases} 0, & \text{if (N is even)} \\ \pm\pi, & \text{if (N is odd)} \end{cases} \tag{3.17}$$

According to eqn. (3.14), the propagator in matrix form $\mathbf{U}(t_c, t_i)$ in eqn. (3.9) reads

$$\mathbf{U}(t_c, t_i) = e^{i\eta} \begin{pmatrix} \cos\alpha & -\sin\alpha \cdot e^{-i\Delta\eta(t_c)} \\ \sin\alpha \cdot e^{i\Delta\eta(t_c)} & \cos\alpha \end{pmatrix} \tag{3.18}$$

$\eta_e(t_c) = \Delta\eta(t' = 0) = \{0, \pm\pi\}$ at $t_c = 0$, thus

$$\mathbf{U}(t_c, t_i) = e^{i\eta} \begin{pmatrix} \cos\alpha & \mp\sin\alpha \\ \pm\sin\alpha & \cos\alpha \end{pmatrix} \tag{3.19}$$

When the time delay t_d extends to $t'_d = t_d + t'$, the corresponding unitary matrix $\mathbf{U}(t', t_c)$ for the field-free propagation from t_c to t' has elements,

$$\mathbf{U}_{kl}(t', t_c) = e^{-iE_k t'/\hbar}\delta_{kl} \tag{3.20}$$

The diagonality implies that $\mathbf{U}(t', t_c)$ has the same block-diagonal structure as $\mathbf{U}(t_c, t_i)$. The total time evolution operator for propagation from t_i via $t_c = 0$ and t' to t'_f is

$$\begin{aligned} \mathbf{U}(t'_f, t_i) &= \mathbf{U}(t'_f, t')\mathbf{U}(t', t_c)\mathbf{U}(t_c, t_i) \\ &= \mathbf{U}(t_f, t_c)\mathbf{U}(t', t_c)\mathbf{U}(t_c, t_i) \end{aligned} \tag{3.21}$$

In the second part of eqn. (3.21), we use the fact that time evolution operator depends only on time intervals but not on initial and final times.

From above we get the following relation

$$\mathbf{U}(t_f, t_c) = \mathbf{U}^{-1}(t_c, t_i) = \mathbf{U}^{\dagger}(t_c, t_i) \tag{3.22}$$

Inserting eqn. (3.22) into (3.21) yields the final coefficients at t'_f,

$$\begin{pmatrix} c_g(t'_f) \\ c_e(t'_f) \end{pmatrix} = \mathbf{U}(t'_f, t')\mathbf{U}(t', t_c)\mathbf{U}(t_c, t_i) \begin{pmatrix} 1 \\ 0 \end{pmatrix} = \begin{pmatrix} \cos^2\alpha + \sin^2\alpha \cdot e^{-i\Delta E t/\hbar} \\ -\cos\alpha\sin\alpha + \cos\alpha\sin\alpha \cdot e^{-i\Delta E t/\hbar} \end{pmatrix}. \tag{3.23}$$

The final population of the excited state is the square of the associated coefficients, and it take the following analytical form

$$P_e(t'_f) = 4P_g(t_c)P_e(t_c) \cdot \left[\frac{1}{2} - \frac{1}{2}\cos\left(\frac{2\pi t'}{T}\right)\right]. \tag{3.24}$$

It varies periodically with amplitude $2P_g(t_c)P_e(t_c)$ and period T. For different time delays $t'_d = t_d + kT/8, k = 1, 2, ..., 7$, the charge migrates between the two degenerate superposition states $(c_g|\Psi_g\rangle + c_e\Psi_e\rangle)$ and $(c_g|\Psi_g\rangle - c_e\Psi_e\rangle)$ with period T.

Within two-state approximation, the laser pulses induce exclusively transitions between the ground state $|\Psi_g\rangle$ and the selective excited target state $|\Psi_e\rangle$ and excludes transition to the other degenerate excited state $|\Psi_{e'}\rangle$. Moreover, the durations of the laser pulses imply sufficiently narrow widths $\Gamma = 0.5\hbar/\tau$ that exclude dipole-allowed one-photon transitions to any other excited states. Therefore, we assume that multi-photon processes to other excited states are negligible and a two-state approximation can be safely used.

To restore the electronic structure symmetry for a three-level system, the pulse $\vec{\epsilon}_b(t)$ for symmetry breaking contains two sub-pulses, which is written as

$$\vec{\epsilon}_b(t) = \sum_{j=1}^{2} \epsilon_{bj} s_{bj}(t) \cdot \left\{ \cos\left[\omega_{ci}(t - t_b)\right] \vec{e}_x + \sin\left[\omega_{ci}(t - t_b)\right] \vec{e}_y \right\}. \tag{3.25}$$

with $s_{bj}(t) = e^{-(t-t_b)^2/2\tau_{bj}^2}$. τ_{bi} and ω_{ci} are the pulse durations and carrier frequencies of two sub-pulses, respectively. The design of two laser pulses for symmetry breaking and restoration will be explained in Subsection 3.2.2. The resulting Hamilton matrix then takes the form

$$\begin{pmatrix} H_{gg} & H_{gm}(t) & H_{ge}(t) \\ H_{mg}(t) & H_{mm} & H_{me}(t) \\ H_{eg}(t) & H_{em}(t) & H_{ee} \end{pmatrix} = \begin{pmatrix} E_g & V_{gm}(t) & 0 \\ V_{gm}^*(t) & E_m & V_{me}(t) \\ 0 & V_{me}^*(t) & E_e \end{pmatrix} \tag{3.26}$$

where

$$V_{kl}(t) = -\frac{1}{\sqrt{2}} d_{kl} \sum_{j=1}^{2} \epsilon_j \left[s_{bj}(t) \cdot e^{i\omega_{cj}(t-t_b)} + s_{rj}(t) \cdot e^{i\omega_{cj}(t-t_r)} \right], kl = \{gm, me\} \tag{3.27}$$

The Hamilton matrix (3.26) satisfies the Hamiltonian condition (3.11) for successful symmetry restoration.

The first pulse $\vec{\epsilon}_b(t)$ partially excites the initial electronic ground state $|\Psi_g\rangle$ via an intermediate state $|\Psi_m\rangle$ to an excited state $|\Psi_e\rangle$ that has a different symmetry as the electronic ground state to break the electronic structure symmetry. The second pulse $\vec{\epsilon}_r(t)$ then de-excites the system from the excited state via the intermediate state back to the electronic ground state to restore the electronic structure symmetry. **Paper** SR1 shows the details of the symmetry breaking and restoration for two models, benzene molecule and ^{87}Rb atom.

3.2.2 Design of Circularly Polarized Pulse

The initial electronic ground state $|\Psi_g\rangle$ and the lowest pair of degenerate excited states are $|\Psi_x\rangle$ and $|\Psi_y\rangle$. Since $|\Psi_x\rangle$ and $|\Psi_y\rangle$ is optically accessible by linearly $x-$ and $y-$polarized laser pulse respectively, we can in principle reach the target excited state $|\Psi_e\rangle$

$$|\Psi_{e+}\rangle = \frac{1}{\sqrt{2}}\left(|\Psi_x\rangle + i|\Psi_y\rangle\right) \tag{3.28}$$

by excitation using a right circularly polarized pulse. Alternatively, the state

$$|\Psi_{e-}\rangle = \frac{1}{\sqrt{2}}\left(|\Psi_x\rangle - i|\Psi_y\rangle\right), \tag{3.29}$$

can be excited via a left circularly polarized pulse. For example, we choose the target excited state $|\Psi_e\rangle = |\Psi_{e+}\rangle$. We set $\vec{\epsilon}_b(t)$ for symmetry breaking as a right circularly polarized laser pulse, which is centered at $t_b < 0$ with amplitude ϵ_b, Gaussian shape $s_b(t)$, duration τ_b and carrier frequency ω_c. The two laser pulses for symmetry breaking $\vec{\epsilon}_b(t)$ and restoration $\vec{\epsilon}_r(t)$ centered at $t_r = -t_b < 0$ are designed as follows

$$\begin{aligned}
\vec{\epsilon_b}(t) &= \Big(\epsilon_{bx}(t), \epsilon_{by}(t), 0\Big) = \epsilon_b s_b(t) \cdot \left(\cos\left[\omega_c(t-t_b)\right], \sin\left[\omega_c(t-t_b)\right], 0\right), \\
\vec{\epsilon_r}(t) &= \big(\epsilon_{rx}(t), \epsilon_{ry}(t), 0\big) = \epsilon_r s_r(t) \cdot \left(\cos\left[\omega_c(t-t_r)\right], \sin\left[\omega_c(t-t_r)\right], 0\right).
\end{aligned} \tag{3.30}$$

with electric field amplitude $\epsilon_r = \epsilon_b$. At time $t = t_b$, $\vec{\epsilon}_b(t)$ has the maximum field strength along $\vec{e}_x$. The resonant carrier frequency ω_c is related to the photon energy $\hbar\omega_c$, and the wavelength $\lambda = cT = 2\pi c/\omega_c$.

$$\begin{aligned}
s_b(t) &= e^{-(t-t_b)^2/2\tau_b^2}, \\
s_r(t) &= e^{-(t-t_r)^2/2\tau_r^2}.
\end{aligned} \tag{3.31}$$

with $\tau_r = \tau_b = \tau$. Thus the total electric field is the sum of two pulses

$$\vec{\epsilon}(t) = \vec{\epsilon}_b(t) + \vec{\epsilon}_r(t). \tag{3.32}$$

Note that the conditions for successful electronic structure symmetry breaking and restoration controlled by attosecond laser pulses require the two attosecond laser pulses must be well separated from each other.

3.2.3 Design of Linearly Polarized Pulse

However, to restore the electronic structure symmetry of atoms and molecules, we can not only use circularly polarized pulse, but also linearly polarized pulse. One can excite the electronic ground state from $|\Psi_g\rangle$ to the excited state $|\Psi_x\rangle$ and $|\Psi_y\rangle$ by linearly $x-$ and $y-$polarized laser pulses, respectively. The first linearly $y-$ polarized pulse centered at $t_b < 0$ is given by

$$\vec{\epsilon}_b(t) = \epsilon_b s_b(t) \cdot \sin\left[\omega_b(t) \cdot (t - t_b) + \eta_b\right] \vec{e}_y. \tag{3.33}$$

The laser carrier frequency may depend on time

$$\omega_b(t) = \omega_c + \omega' \cdot (t_b + t) \tag{3.34}$$

where ω_c is the resonant carrier frequency, and the parameter ω' allows applications to various scenarios with linear up-chirp ($\omega' > 0$), zero chirp ($\omega' = 0$), or down-chirp ($\omega' < 0$). The second laser pulse $\vec{\epsilon}_r(t)$ for symmetry restoration centered at $t_r = -t_b > 0$ is designed as $time - reversed$ copy of the pulse that breaks symmetry,

$$\vec{\epsilon}_r(t_r - t) = \vec{\epsilon}_b(t + t_b), \tag{3.35}$$

and

$$\vec{\epsilon}_r(t) = -\epsilon_b s_r(t) \cdot \sin\left[\omega_r(t) \cdot (t - t_r)\right] \vec{e}_y, \tag{3.36}$$

where

$$\omega_r(t) = \omega_c - \omega' \cdot (t - t_r), \tag{3.37}$$

The total electric field of the two laser pulses $\vec{\epsilon}(t)$ is, therefore, time-reversible,

$$\vec{\epsilon}(t) = \vec{\epsilon}(-t) \tag{3.38}$$

The matrix representation of the Hamiltonian $H(t)$ in eqn. (3.7) is, therefore, also time reversible,

$$\mathbf{H}(t) = \mathbf{H}(-t). \tag{3.39}$$

For linearly polarized laser pulses, the matrix representations are real-valued, thus

$$\mathbf{H}(t) = \mathbf{H}^*(-t) \tag{3.40}$$

which satisfies the Hamiltonian condition in eqn. (3.11) for successful symmetry breaking and restoration coherent controlled by ultrafast attosecond laser pulse.

According to eqn. (3.18), the time delay t_d has to be properly chosen such that the coefficients at $t_c = 0$ is real-valued. Therefore, the phase difference at t_c is

$$\Delta\eta(t') = \eta'_e - \eta'_g - \Delta E \cdot t'/\hbar, \text{modulo } 2\pi = \begin{cases} 0 & \text{if } t_d = NT(\text{N is even}) \\ \pm\pi & \text{if } t_d = NT(\text{N is odd}) \end{cases}. \tag{3.41}$$

For various time delays $t'_d = t_d + kT/8, k = 1, 2, ..., 7$, instead of restoring the electronic structure symmetry at the ground state, we observe the charge migration between two degenerate superposition states $(c_g|\Psi_g\rangle + c_e|\Psi_y\rangle)$ and $(c_g|\Psi_g\rangle - c_e|\Psi_y\rangle)$ with period T. The final population of the excited state also varies periodically as a function of the chosen time delay, as implied by eqn. (3.24).

The first linearly y-polarized pulse or chirp pulse $\vec{\epsilon}_b(t)$ breaks the electronic structure symmetry by exciting a system from the electronic ground state $|\Psi_g\rangle$ to a superposition state $(c_g|\Psi_g\rangle + c_e|\Psi_y\rangle)$, which has a different symmetry from the ground state. The second pulse $\vec{\epsilon}_r(t)$ stops the ultrafast charge migration at a proper time t_r and successfully restores the electronic structure symmetry by de-exciting the superposition state back to the electronic ground state. **Paper** SR2 shows the application of symmetry breaking and restoration in benzene molecule controlled by linearly polarized pulse.

3.2.4 Numerical Propagator

For solving the TDSE, there exist various ways,[113] which range from direct numerical integration using e.g. Runge-Kutta[114] to the Split-operator method[115] and Krylov-Subspace techniques.[116, 117] For the purpose of symmetry restoration, it is important that the propagator of the wave packet is strictly unitary (see eqns. (3.10), (3.12)). Further, it requires an accuracy on the attosecond timescale. But all existing propagators do not satisfy both these two conditions. Hence, we have developed a strictly unitary spectral propagator that meets the tight accuracy requirements for symmetry restoration.

The numerical propagation from the initial coefficients $\mathbf{c}(t_i)$ to the final coefficients $\mathbf{c}(t_f)$ is carried out on an evenly spaced temporal grid $t_i, t_i + \Delta t, ..., t_k, t_k + \Delta t, ..., t_f$, with attosecond time step Δt,

using the approximations

$$\begin{aligned}\mathbf{c}(t_f) &\approx \prod_k \hat{T} e^{-i\int_{t_k}^{t_k+\Delta t} dt' H(t')/\hbar}\mathbf{c}(t_i) \\ &\approx \prod_k \hat{T} e^{-iH(t_k+\Delta t/2)\Delta t/\hbar}\mathbf{c}(t_i) \\ &\approx \prod_k \hat{T} V^{\dagger}(t_k+\Delta t/2) e^{-iE(t_k+\Delta t/2)\Delta t/\hbar} V(t_k+\Delta t/2)\mathbf{c}(t_i).\end{aligned} \tag{3.42}$$

Here $H(t_k + \Delta t/2)$ is the Hamiltonian matrix at the center of the time interval $[t_k, t_k + \Delta t]$. It is diagonalized either analytically for a two-level system or numerically using the routine *zheev* of LAPACK otherwise. The resulting eigenenergies at time $t_k + \Delta t/2$ are stored in a diagonal matrix $E(t_k + \Delta t/2)$; the matrix $V(t_k + \Delta t/2)$ contains the eigenvectors. Hamiltonian condition in eqn. (3.11) and time delay conditions in eqn. (3.17), (3.41) and (3.49) are two sufficient conditions for successful symmetry breaking and restoration coherent controlled by ultrafast attosecond laser pulse. To make the symmetry restoration numerically successful, one has to adjust time delay t_d with a precision of a few attoseconds and it should be short enough to avoid the decoherence effect due to nuclear motion.

3.3 Extended Theory for Symmetry Restoration at the Excited State

The final population of excited state that is shown in eqn. (3.24) demonstrates that we can also restore the electronic structure symmetry at the excited state once the symmetry of $|\Psi_e\rangle$ is same as the ground state. Namely, after the first laser pulse breaks the symmetry of the initial electronic ground state by exciting it to the superposition state, we find that the second laser pulse can also restore the symmetry by exciting the superposition state further to the pure excited state, if the electronic structure symmetry of excited state belongs to the same symmetry point group as the ground state. In this context, we interpret symmetry restoration as redistributing the electronic structure such that the electronic structure symmetry can be reassigned into the initial symmetry point group by creating a pure IRREP in a given group. For complete population transfer, the pulse has to be a resonant π-pulse.[4, 112] This suggests the concept that

$$\text{first laser pulse} \; + \; \text{second laser pulse} = \text{resonant } \pi-\text{pulse}. \tag{3.43}$$

This condition holds irrespectively of the polarizations of the laser pulses, namely they can be linearly x- or y-polarized, or circularly right (+) or left (-) polarized. The resonant condition means that the photon energy $\hbar\omega$ matches the energy gap between the ground and excited states. For this purpose,

the second laser pulse $\vec{\epsilon}_r(t)$ in eqn. (3.30) has to be designed such that its electric field at t_r is along the same polarization as t_b. For the case of a circularly polarized pulse in an ideal two-level system, we get the following conditions

$$\begin{aligned} t_r &= -t_b = NT/2, N = 1, 2, 3... \\ t_d &= t_r - t_b = NT, N = 1, 2, 3.... \end{aligned} \tag{3.44}$$

The two pulses for symmetry breaking and restoration in the excited state are then designed as

$$\begin{aligned} \vec{\epsilon_b}(t) &= \epsilon_b s_b(t) \cdot (\cos\left[\omega_c(t - t_b)\right], \sin\left[\omega_c(t - t_b)\right], 0), \\ \vec{\epsilon_r}(t) &= \epsilon_r s_r(t) \cdot (\cos\left[\omega_c(t - t_r)\right], \sin\left[\omega_c(t - t_r)\right], 0) \\ &= \epsilon_r s_r(t) \cdot (\cos\left[\omega_c(t - t_b)\right], \sin\left[\omega_c(t - t_b)\right], 0). \end{aligned} \tag{3.45}$$

The total electric field again takes the form

$$\begin{aligned} \vec{\epsilon}(t) &= \vec{\epsilon_b}(t) + \vec{\epsilon_r}(t) \\ &= \left[\epsilon_b s_b(t) + \epsilon_r s_r(t)\right] \cdot (\cos\left[\omega_c(t - t_b)\right], \sin\left[\omega_c(t - t_b)\right], 0). \end{aligned} \tag{3.46}$$

For a complete population transferring from ground state $|\Psi_g\rangle$ to an excited state $|\Psi_e\rangle = |\Psi_{e+}\rangle$ by two laser pulses, which means that

$$\begin{aligned} & d\left[\epsilon_b \int_{t_i}^{t_f} dt' s_b(t') + \epsilon_r \int_{t_i}^{t_f} dt' s_r(t')\right] / \sqrt{2}\hbar \\ &= \sqrt{\pi} d(\epsilon_b \tau_b + \epsilon_r \tau_r)/\hbar \\ &= \sqrt{\pi} d\epsilon_\pi \tau_\pi / \hbar \\ &= \pi/2, \end{aligned} \tag{3.47}$$

It implies that the product $\epsilon_\pi \tau_\pi$ of the field amplitude times the parameter for the duration of the π pulse yields the same results as the combination of two laser pulses. The concept in eqn. (3.43) can be rewritten as

$$\epsilon_b \tau_b + \epsilon_r \tau_r = \epsilon_\pi \tau_\pi. \tag{3.48}$$

If the first resonant right (+) circularly polarized laser pulse with field amplitude ϵ_b, with Gaussian shape function $s_b(t)$, duration τ_b for breaking the electronic structure symmetry of the ground state, then one can employ the second resonant right (+) circularly polarized laser pulse with field amplitude $\epsilon_r = \epsilon_\pi - \epsilon_b$ with Gaussian shape function $s_r(t)$ and the same duration $\tau_r = \tau_b$ to restore symmetry at the electronic excited state. According to eqn. (3.44), to restore the symmetry in the excited state

successfully, the phase difference at t_c should be

$$\begin{aligned} &\eta_g(t_c) = 0, \\ &\Delta\eta_e(t_c) = \eta_e(t_c) \ \text{ modulo } \ 2\pi = \begin{cases} -\pi/2 \ \text{ if } \ N = 1,3,5,...(\text{odd}) \\ +\pi/2 \ \text{ if } \ N = 2,4,6,...(\text{even}) \end{cases} \end{aligned} \tag{3.49}$$

It demonstrates that the success again depends on the time delay between the laser pulses, which implies that the time delay t_d must be equal to an integer number N of the period T of charge migration. As a convention, we set $\eta_g(t_c) = 0$. From eqn. (3.14), the coefficients at t_c can be written as

$$\begin{pmatrix} c_g(t_c) \\ c_e(t_c) \end{pmatrix} = \begin{pmatrix} \cos\alpha \\ \pm i\sin\alpha \end{pmatrix}. \tag{3.50}$$

According to eqn. (3.18), we can obtain the corresponding unitary matrix $\mathbf{U}(t_c, t_i)$, for propagating the initial coefficients $c(t_i)$ to $c(t_c)$

$$\mathbf{U}(t_c, t_i) = \begin{pmatrix} \cos\alpha & \pm i\sin\alpha \\ \pm i\sin\alpha & \cos\alpha \end{pmatrix}. \tag{3.51}$$

The first column of the matrix in eqn. (3.51) is imposed by the coefficients in eqn. (3.50), the second column is due to the unitarity of $\mathbf{U}(t_c, t_i)$. Since here we want to restore the electronic structure symmetry at the excited state at final time t_f, namely $|c_e(t_f)|^2 = 1$. Therefore, the unitary matrix for propagating the system from the initial time t_i to the final time t_f is

$$\mathbf{U}(t_f, t_i) = e^{i\eta_{ef}} \begin{pmatrix} 0 & 1 \\ 1 & 0 \end{pmatrix} \tag{3.52}$$

with irrelevant phase factor $e^{i\eta_{ef}}$. Moreover, the evolution operator $\mathbf{U}(t_f, t_i)$ can be divided into two parts for symmetry breaking and restoration

$$\mathbf{U}(t_f, t_i) = \mathbf{U}(t_f, t_c)\mathbf{U}(t_c, t_i) \tag{3.53}$$

Inserting eqn. (3.51) and (3.52) into eqn. (3.53) yields the evolution operator for propagating the system

from t_c to t_f,

$$\mathbf{U}(t_f, t_c) = e^{i\eta_{ef}} \begin{pmatrix} \pm i \sin\alpha & \cos\alpha \\ \cos\alpha & \pm i \sin\alpha \end{pmatrix}. \tag{3.54}$$

For various time delays $t'_d = t_d + kT/8, k = 1, 2, ..., 7$, the final coefficients at time $t'_f = t_f + t'$ are then obtained as

$$\begin{pmatrix} c_g(t'_f) \\ c_e(t'_f) \end{pmatrix} = \mathbf{U}(t'_f, t')\mathbf{U}(t', t_c)\mathbf{U}(t_c, t_i) \begin{pmatrix} 1 \\ 0 \end{pmatrix} = \begin{pmatrix} -\cos\alpha \sin\alpha (1 - e^{i\eta'}) \\ \cos^2\alpha + \sin^2\alpha \cdot e^{i\eta'} \end{pmatrix}. \tag{3.55}$$

As a function of the time delays, the final population of the excited state

$$\begin{aligned} P_e(t'_f) = |c_e(t'_f)|^2 &= \left(\cos^2\alpha + \sin^2\alpha \cdot e^{i\eta'}\right) \cdot \left(\cos^2\alpha + \sin^2\alpha \cdot e^{-i\eta'}\right) \\ &= 1 - 2\cos^2\alpha \sin^2\alpha (1 - \cos\eta') \\ &= 1 - 2P_g(t_c)P_e(t_c)\left[1 - \cos(\frac{2\pi t'}{T})\right]. \end{aligned} \tag{3.56}$$

various periodically with amplitude $2P_g(t_c)P_e(t_c)$ and period T, with comparison with eqn. (3.24).

The first laser pulse breaks the electronic structure symmetry by exciting the electronic ground state $|\Psi_g\rangle$ to a superposition state of the ground and an excited state $|\Psi_e\rangle$. The second laser pulse stops the charge migration and restore the electronic structure symmetry via excitation of the superposition state and completely to a pure excited state. For successful symmetry restoration, the time delay between the two peaks of two laser pulses has to be chosen as the integer number of the charge migration period in few attosecond precision.

Chapter 4

Publications

The following chapter demonstrates the academic publications, which are the main of the dissertation. The publications consist of published articles and book chapters. They can be classified into two themas:

- **SR** Ultrafast laser control molecular and atomic symmetry breaking and restoration
- **CM** Charge migration process

Paper SR1

"Attosecond Control of Restoration of Electronic Structure Symmetry"

C. Liu, J. Manz, K. Ohmori, C. Sommer, N. Takei, J. C. Tremblay, and Y. Zhang

Phys. Rev. Lett. **121**, 173201 (2018)

DOI: 10.1103/PhysRevLett.121.173201

URL: http://dx.doi.org/10.1103/PhysRevLett.121.173201

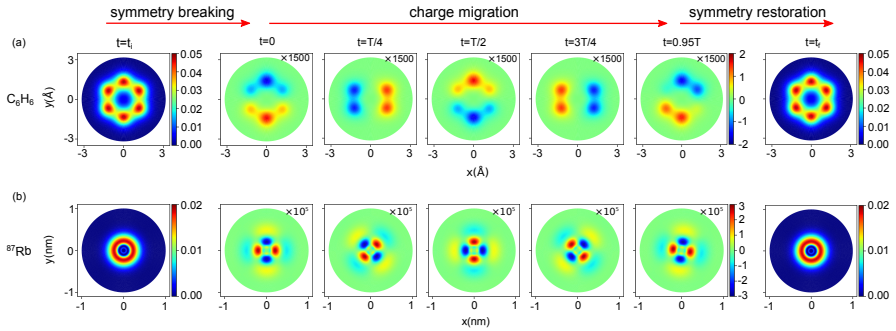

Figure 4.1: Graphical Abstract. Reprint with permission from Liu et al. SR1 (©2018 American Physical Society)

Author contributions

The project was suggested by Jörn Manz and he also did most of the conceptual theory. Jean Christophe Tremblay generated the propagator. Kenji Ohmori, Nobuyuki Takei, Yichi Zhang and Christian Sommer did the Ramsey interferometry experiment for ^{87}Rb atom. I did the numerical calculations for benzene molecule and ^{87}Rb atom, with energy levels and transition dipole moments of ^{87}Rb atom from Nobuyuki Takei. I prepared all the figures, with the snapshots of benzene molecule from Jean Christophe Tremblay and the snapshots of ^{87}Rb atom from Nobuyuki Takei, the graphical method Concerning the snapshots for the ^{87}Rb atom was developed by Christian Sommer and Nobuyuki Takei. All coauthors discussed the final results. The zero draft manuscript for theoretical part was written by Jörn Manz and our experimental partners wrote the experimental part for ^{87}Rb atom. All coauthors contributed to the final version of this manuscript.

Paper SR2

"From Molecular Symmetry Breaking to Symmetry Restoration by Attosecond Quantum Control, In: Yamanouchi K., Martin P., Sentis M., Ruxin L., Normand D. (eds) Progress in Ultrafast Intense Laser Science XIV"

C. Liu, J. Manz, and J. C. Tremblay

Springer Series in Chemical Physics, Springer, Cham vol.**118**, 117-141 (2018)

DOI: 10.1007/978-3-030-0376-4

URL: http://dx.doi.org/10.1007/978-3-030-0376-4

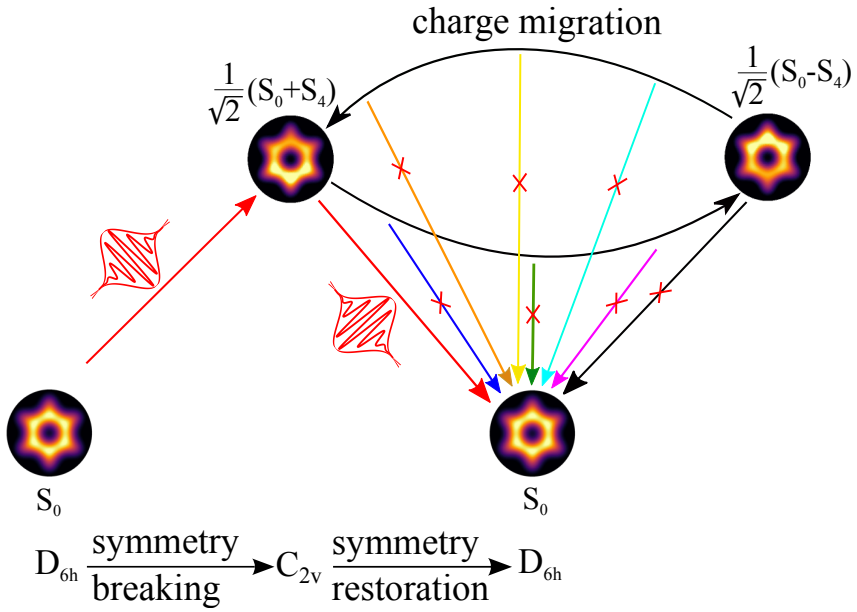

Figure 4.2: Graphical Abstract. Reprint with permission from Liu et al. (©Springer Nature Switzerland AG 2018)

Author contributions

The project was suggested by Jörn Manz and he also did most of the conceptual theory. Jean Christophe Tremblay plotted the snapshots. I did the numerical calculations based on the numerical propagator in **Paper** SR1 and prepared all the figures. All coauthors discussed the final results. The manuscript was predominantly written by Jörn Manz. All coauthors contributed to the final version of this manuscript. In addition, I presented the results at the conference "11th Triennial Congress of the World Association of Theoretical and Computational Chemists" in Munich, and won one of the nine "The Best Poster" from more than 900 were posters presented at the conference.

Paper SR3

"From Symmetry Breaking via Charge Migration to Symmetry Restoration in Electronic Ground and Excited States: Quantum Control on the Attosecond Time Scale"

C. Liu, J. Manz, and J. C. Tremblay

Appl. Sci. **9**, 953 (2019)

DOI: 10.3390/app9050953

URL: http://dx.doi.org/10.3390/app9050953

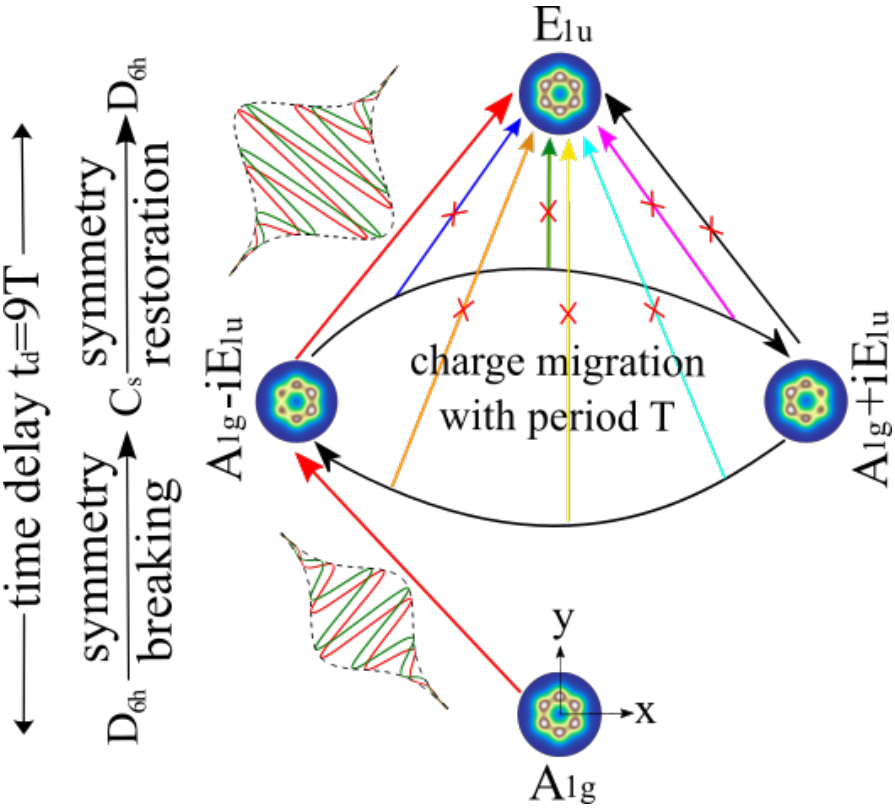

Figure 4.3: Graphical Abstract. Reprint with permission from Liu et al. (©2019 by the authors. Licensee MDPI, Basel, Switzerland.)

Author contributions

Jean Christophe Tremblay and Jörn Manz proposed the new strategy of quantum control of electronic structure symmetry breaking and restoration. Jörn Manz discovered the concept, derived most part of the theory and wrote the zero draft manuscript. I obtained the analytical expression of the population of excited state, carried out all quantum dynamics simulations and prepared all the figures (the snapshots of the one-electron density were plotted by Jean Christophe Tremblay). All coauthors discussed the final results. All coauthors contributed to the final version of this manuscript.

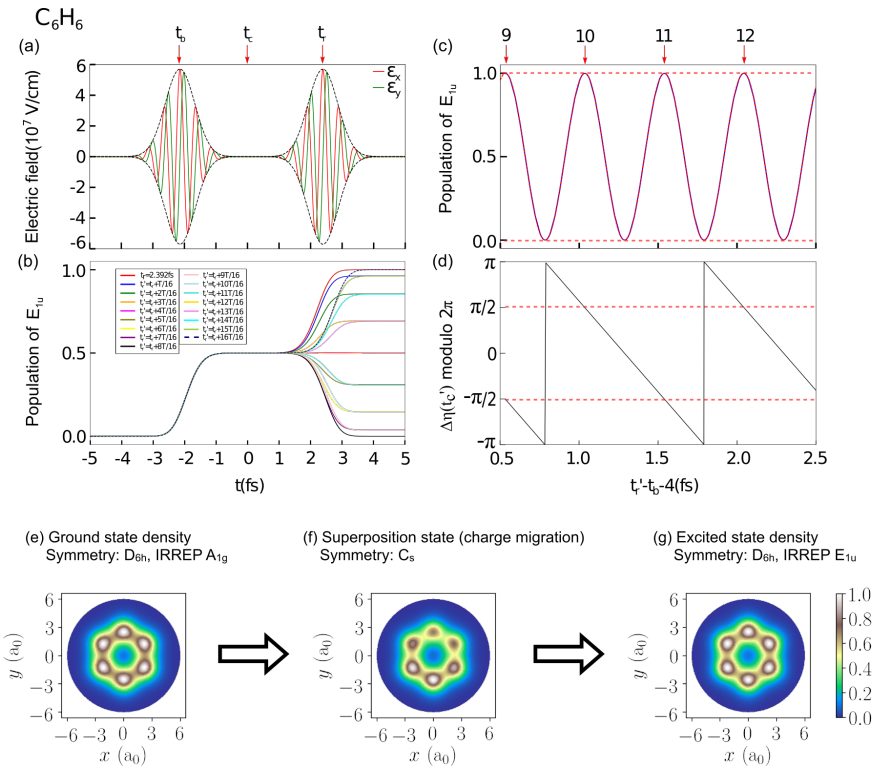

Figure 4.4: Graphical Abstract. Reprint with permission from Bacic et al. (©The Royal Society of Chemistry 2018)

Paper SR4

"Molecules in confinement in clusters, quantum solvents and matrices: general discussion"

Z. Bacic et al

Faraday Discuss. **212**, 569-601 (2018)

DOI: 10.1039/C8FD90053A

URL: http://dx.doi.org/10.1039/C8FD90053A

Author contributions

The project was suggested by Jörn Manz and he also did most of the conceptual theory. Jean Christophe Tremblay plotted the snapshots. I did the numerical simulations based on the numerical propagator in **Paper** SR1 and prepared all the figures. I presented the results in the conference - Faraday Disscusion. All coauthors discussed the final results. The manuscript was predominantly written by Jörn Manz. All coauthors contributed to the final version of this manuscript.

Paper CM1

"Multidirectional Angular Electronic Flux during Adiabatic Attosecond Charge Migration in Excited Benzene"

G. Hermann, **C. Liu**, J. Manz, B. Paulus, J. F. Pérez-Torres, V. Pohl, and J. C. Tremblay

J. Phys. Chem. A **120**, 5360-5369 (2016)

DOI: 10.1021/acs.jpca.6b01948

URL: http://dx.doi.org/10.1021/acs.jpca.6b01948

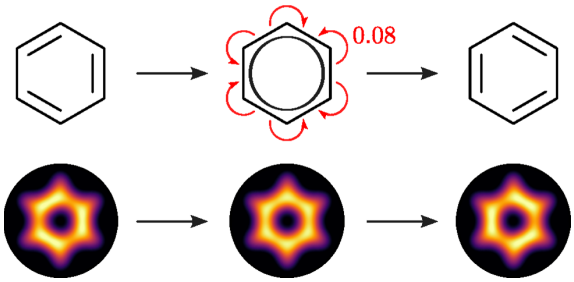

Figure 4.5: Graphical Abstract. Reprint with permission from Hermann et al. (©2016 American Chemical Society)

Author contributions

The research framework of this work was outlined by Jörn Manz and Jhon Fredy Pérez-Torres. Jhon Fredy Pérez-Torres did preliminary CI calculations. I prepared preliminary results and prepared the preliminary figures for the novel methodology. Vincent Pohl performed the CASSCF calculations, which are presented in the final version of the paper, with input from Beate Paulus and Jean Christophe Tremblay. The final result used in the paper was done by Gunter Hermann and Vincent Pohl. They also prepared the figures for the publication. All authors were involved in the concluding discussion of the results and contributed to the final version of the manuscript, which was mainly written by Jörn Manz.

Paper CM2

"Attosecond Angular Flux of Partial Charges on the Carbon Atoms of Benzene in Non-Aromatic Excited State"

G. Hermann, **C. Liu**, J. Manz, B. Paulus, V. Pohl, and J. C. Tremblay

Chem. Phys. Lett. **683**, 553-558 (2017)

DOI: 10.1016/j.cplett.2017.01.030

URL: http://dx.doi.org/10.1016/j.cplett.2017.01.030

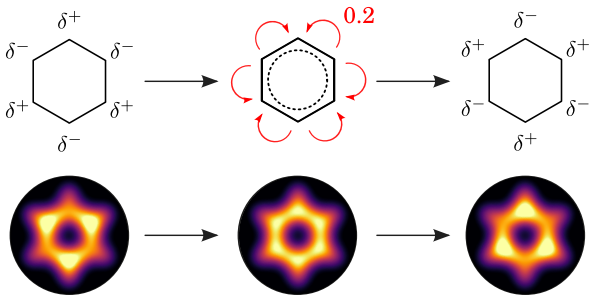

Figure 4.6: Graphical Abstract. Reprint with permission from Hermann et al. (©2017 Elsevier B.V. All rights reserved.)

Author contributions

The idea behind this work was conceived by Jörn Manz. Vincent Pohl and Gunter Hermann performed the CASSCF calculations with input from Beate Paulus and Jean Christophe Tremblay. I applied the methodology of **Paper** CM1 and prepared results for the comparison to the new improved methodology. Based on this program Vincent Pohl and Gunter Hermann implemented the new improved methodology, and prepared the final results. The first version of the manuscript was written by Jörn Manz. All coauthors contributed to the final version of this manuscript.

Chapter 5

Summary

This chapter gives a brief summary of the key results of the academic publications contained in the context, which is divided into two topics:
(i) attosecond coherent control of electronic structure Symmetry breaking and Restoration (SR) in atoms and molecules;
(ii) laser control of attosecond ultrafast Charge Migration (CM).

As will be illustrated below, the primary topic is intimately connected to charge migration. This dissertation aims at developing a general theory of coherent control electronic structure symmetry breaking and restoration by ultrashort laser pulses, with applications in two models: benzene molecule (with highly symmetric electronic ground state) and ^{87}Rb Rydberg atom (with highly symmetric isotropic ground state). There are four strategies of attosecond control symmetry breaking and restoration of electronic structure in atoms and molecules developed in this dissertation. **Paper** SR1 refers Strategy 1, which shows the theory of attosecond control electronic structure symmetry breaking and restoration in electronic ground state by means of two identical circularly polarized pulses. **Paper** SR2 refers Strategy 2, which represents that two time-reversed copy of linearly polarized pulses drive symmetry breaking and restoration in electronic ground state. **Paper** SR3 refers Strategy 3, which demonstrates that two general pulses can be used for attosecond control of symmetry breaking in electronic ground state but symmetry restoration in excited state. **Paper** SR4 refers Strategy 4, which implies the possibility of restoring the electronic structure symmetry twice during one charge migration period. In the following context, I will go through these four strategies. For convenience, symmetry breaking and restoration in the following context all refer to symmetry breaking and restoration of the electronic structure.

Ulusoy and Nest [49] demonstrated that well-designed laser pulses can control the aromaticity of oriented benzene molecule, for which they selectively excited two non-aromatic electronic superposition states of the benzene molecule by applying optimal control theory. This work motivated us to control the electronic structure symmetry of the benzene molecule via laser excitation. We assume that the

atomic centers of the molecule are placed in the laboratory $xy-$plane, with the nuclei frozen at their equilibrium geometry such that two of the carbon nuclei located on the $y-$axis. The $x-$axis is defined as the direction of the field with maximum amplitude. The electronic ground state has $IRREP = A_{1g}$ in D_{6h} symmetry point group.

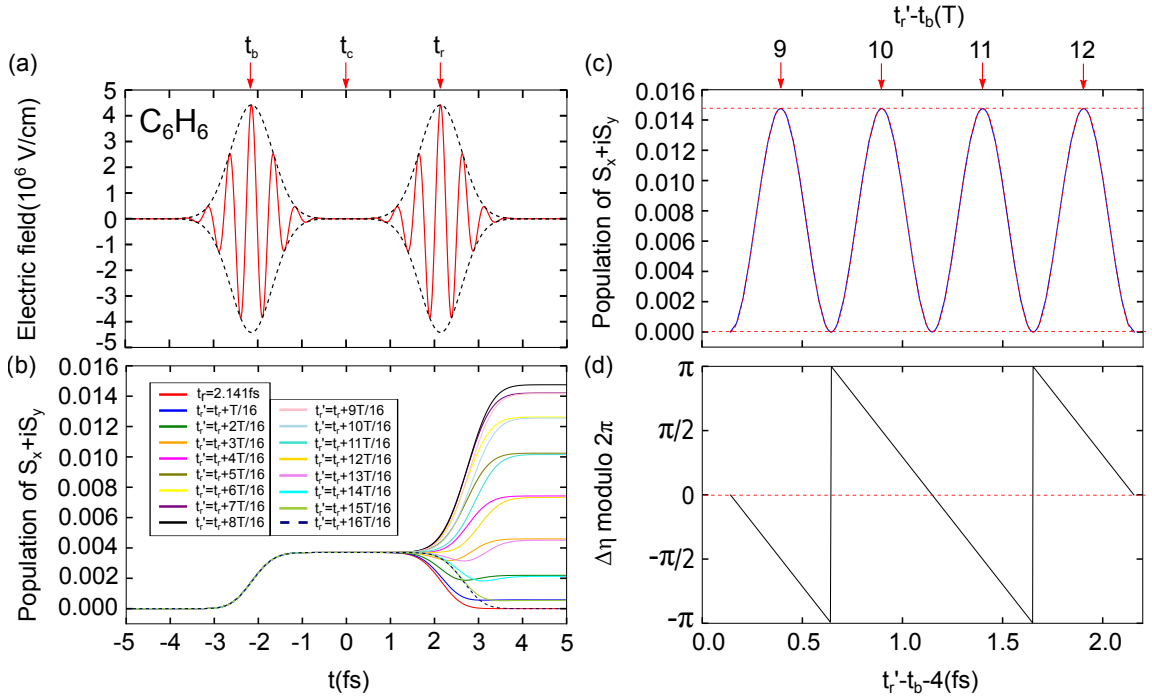

Figure 5.1: Attosecond control symmetry breaking and restoration in benzene molecule by y-circularly polarized pulses. (a) Envelope and x-component of two laser pulses centered at t_b and t_r for symmetry breaking and restoration, respectively. (b) Evolution of final population of the excited state for various time delays. (c) Final population of the excited state versus time delay. (d) Phase difference at temporal central time between wave functions of the ground state and excited state. The figure is adapted from **Paper** SR1.

Our target excited state is a complex-valued superposition state of two real-valued degenerate excited states, which are optically accessible by right or left-circularly polarized pulses. The degenerate excited states have $IRREP = E_{1u}$ in D_{6h} symmetry point group. For achieving attosecond control symmetry restoration, we design two identical ultrashort few-cycle transform limited circularly polarized pulses in **Paper** SR1, e.g. two pulses have same polarizations, Gaussian envelops, amplitudes, carrier frequencies and durations. The pulse durations of two laser pulses for symmetry breaking and restoration have to be short enough to avoid the effect of nuclear motion, and they have to be separated well such that around the central time t_c (see Fig. 5.1a) is a quasi-field-free environment. The mean durations of the pulses are $\Delta\tau = 0.403\, fs$ and the error of the excitation energy is $\Delta E = 0.817\, eV$, therefore, the target state is the only one that can be excited from the electronic ground state, according to one-photon transition. Thus we assume that multiphoton processes are negligible and two-state approximation is safely applied. In this representation the matrix of the system Hamiltonian with

semiclassical coupling with the laser field is adjunct upon time reversal.

We design the first right-circularly polarized laser pulse for symmetry breaking centered at $t_b < 0$ (see Fig. 5.1a), which excites 0.37% population of the electronic ground state to an excited state, and a superposition is created. The IRREP of the superposition state can no longer be assigned to the original symmetry point group D_{6h}, but belongs to C_s symmetry point group — a subgroup of D_{6h}, which means the symmetry breaking from D_{6h} to C_s. Since the superposition state is not an eigenstate of the system, it documents ultrafast attosecond circular charge migration between two degenerate superposition states with period $T = 504as$ for the benzene molecule. The period depends on the energy difference between the electronic ground state and the target excited state. The larger energy gap is, the faster charge migrates. Without external interactions, the ultrafast attosecond charge migration will last for very long time between two degenerate superposition states.

Note that in the case of the benzene molecule, this period will be affected by the choice of electronic structure method and basis set. For ^{87}Rb atom, the energy scale (and the time difference) was determined experimentally. The second identical right-circularly polarized laser pulse is designed to be centered at $t_r = -t_b > 0$ (see Fig. 5.1a) to stop the ultrafast attosecond charge migration and restore the symmetry in the electronic ground state by de-exciting the superposition state back to the initial state with a proper time delay t_d. Here, time delay $t_d = t_r - t_b$ is defined to be the time difference between the peaks of two laser pulses. A semiclassical formula is derived to describe the motion of the electron charge and analyze the time-delayed two-photon process. The population of the excited state can go back to zero depending on the time delay, which can be rather long.

The success of symmetry restoration depends on the time delay in few attoseconds precision such that the phase difference at central time t_c is 0 or $\pm\pi$. For few attoseconds precision, we are required to develop strict unitary numerical propagator, which is explained in Section 3.2.4. The mechanism of laser control symmetry breaking and restoration is illustrated in Fig. 5.1. Only when the time delay is chosen as $t_d = \left(N + \frac{1}{2}\right) T$, ($N$ is integer number) such that the wave function is real-valued at the central time with phase difference is 0 or $\pm\pi$, one can switch off the ultrafast attosecond charge migration and successfully achieve the symmetry restoration in electronic ground state for possibility close to 100%. All other time delays document the ultrafast attosecond charge migration between two degenerate superposition states, and correspond to different final populations of the excited state as shown in Fig. 5.1b. The final population of the excited state varies periodically with amplitude $2P_g(t_c)P_e(t_c)$ and period T. Numerical results are plotted for comparison with the analytical results, which denotes a very good agreement as shown in Fig. 5.1c. In the quasi-field-free environment near the central time, the superposition state evolves field freely and the related populations of the

electronic ground state and target excited state are constant. The phase difference at the central time decreases linearly (modulo 2π) with time, which is shown in Fig. 5.1d.

another application of the same theory of attosecond control symmetry breaking and restoration is in ^{87}Rb atom, which is motivated by various fundamental effects that have been discovered for the system. For this purpose, a two-photon excitation and three-level system is applied. Two identical right-circularly polarized pulses are required for the processes of symmetry breaking and symmetry restoration, and each pulse contains two sub-pulses. The first laser pulse non-resonantly excites 0.37% population of the ^{87}Rb atom from its initial state $5^2S_{1/2,F=2,m_F=2}$ with isotropic electronic structure via an intermediate state $5^2P_{3/2,F=3,m_F=3}$ to an excited state $42^2D_{5/2,F=4,m_F=4}$ and a superposition state with anisotropic structure is recreated. It reveals symmetry breaking, which is monitored by measuring the nonzero population of the excited state. The superposition state documents the ultrafast attosecond charge migration with period $T = 992\ as$ for ^{87}Rb atom. The second laser pulse achieves the reverse process of de-exciting the superposition state via the intermediate state back to the initial ground state, which implies the symmetry restoration. The first pulse induces off-resonant transition from the ground state to intermediate state to avoid the population localization. The theoretical results are confirmed for ^{87}Rb atom by a high contrast Ramsey interferometry measurement of the dependence of the population of the excited state on time delay. The details of Ramsey interferometry experiment are written in supplementary materials of **Paper** SR1. For this strategy of attosecond control symmetry breaking and restoration in the electronic ground state, traditional femtosecond pump-probe pulses are not suited for such interferometry experiments. Note that in this excitation process, we shall use a weak laser, since the very high intensity may cause secondary effect such as multiphoton excitations or ionization on ^{87}Rb atom.

For visualizing the process of symmetry breaking and restoration, we analyze the N-electron dynamics generated by the electronic continuity equation. The final population of the excited state and the phase difference for ^{87}Rb atom follow the same rules as for the benzene molecule. In these two applications, the excitation is only 0.37%, but the phenomenon of symmetry breaking and restoration is clearly visualized by the snapshots of one-electron density proof-of-principle. The theoretical prediction of symmetry restoration for ^{87}Rb atom is confirmed by a high contrast Ramsey interferometry experiment by measuring the time-delay dependence of the final population of the excited Rydberg state with $\pm 3\ as$ precision. However, the $\pm 3\ as$ time resolution in 50 ps time domain still induces an error between experimental observation and theoretical results. In this experiment, the experimental contrast of the Ramsey interferogram is about 0.94, where the contrast is defined to be the ratio of the amplitude of the fitted sinusoidal function to its mean value. The high contrast denotes that almost all

the population in the excited state is de-excited back to the symmetric ground state for specific time delays, for which the phase difference is 0 or $\pm\pi$. This means that a very small inaccuracy in respecting of the conditions for symmetry restoration induce a large experimental error. The experiment can observe the period and measure the excited state population and keep very high contrast 0.94 with ± 3 *as* time resolution even when two pulses are separated by 50 *ps*.

In **Paper** SR1, we originally establish a basic theory of attosecond control symmetry breaking and restoration of electronic structure in atoms and molecules. For this purpose, we derive two sufficient conditions for successful symmetry restoration numerically:
(i) the Hamiltonian must be adjunct upon time revesal;
(ii) the phase difference at the central time is 0 or $\pm\pi$.
This work for the first time demonstrates that the laser pulse can not only break the symmetry but can also restore the symmetry theoretically and experimentally. **Paper** SR1 gives an analytical formula for the time evolution of the final population of the excited state and the dependence of the phase difference on the time delay. This strategy also serves as a switch of the ultrafast attosecond charge migration by manipulating the time delay between two pulses. The experiment reveals that control the phase factor with attosecond precision is almost sufficient to reach the theoretical condition for symmetry restoration.

Based on the theory and conditions of successful symmetry breaking and restoration for the benzene molecule and ^{87}Rb atom that we have derived in **Paper** SR1, Strategy 2 in **Paper** SR2 shows that linearly and chirped pulses are also be used for symmetry breaking and restoration in the ground state. The target excited state is excited eigenstate which can be accessed via linearly x-polarized or y-polarized pulse. Two linearly y-polarized pulses are designed as time-reversed copy of each other. The first linearly y-polarized pulse breaks the symmetry by resonantly exciting 50% population of the ground state (with $IRREP = A_{1g}$ in D_{6h} symmetry point group) to an excited state (with $IRREP = E_{1u}$ in D_{6h} symmetry point group) and a superposition state (with C_{2v} symmetry) is prepared, which initiates attosecond ultrafast charge migration with period $T = 504$ *as*. We can easily recognizes its C_{2v} symmetry from the snapshots of one-electron density in Fig. 5.2 (top-left), with part of electronic density localized on the "south pole". The second time-reversed copy of linearly y-polarized pulse is applied to switch off the ultrafast attosecond charge migration, and restore the symmetry by de-exciting the superposition state back to its initial ground state with a proper time delay such that the phase difference is 0 or $\pm\pi$ at the central time. This implies that the wave function at the central time is real-valued, which means zero electronic fluxes, e.g. no charge migration occurs at the specific time. Namely, one can restore the symmetry in electronic ground state only from the

target superposition state when the electron charges are localized on "south pole". The red arrow in Fig. 5.2 refers the success case of coherent control symmetry breaking and restoration in the ground state. The black round arrows refer to attosecond charge migration process between two degenerate superposition states with charge migration period $T = 504\ as$. The other seven color arrows refer to failed cases of coherent control symmetry restoration in ground state. For various time delays, the final population of the excited state varies periodically with amplitude $2P_g(t_c)P_e(t_c)$ and period T, and the phase difference at the central time (modulo 2π) decreases linearly with time.

For the purpose of exciting 50% of the population of the ground state, these two laser pulses must be designed as $\frac{\pi}{2}$-laser pulses. The difference between SR2 and SR1 is that two pulses used here in SR2 are time-reversed copy of linearly polarized pulses, instead of two identical circularly polarized pulses in **Paper** SR1. In addition, the laser pulse is no longer required to take a Gaussian shape and can be more intensive than the pulses we used in **Paper** SR1. The pulse durations of the ultrashort intense linearly $y-$polarized pulses for symmetry breaking and restoration should be very short so that the entire propagation time is within 10 fs, where the effect of nuclear dynamics on the laser driven electronic dynamics of benzene can be neglected. For our case, the two laser pulses are ultrashort few cycle transform limited pulses. Since the maximum of the intensity (5.873 TW/cm^2) is still below the typical intensity required for multiphoton ionization, thus the ionization process can also be neglected.

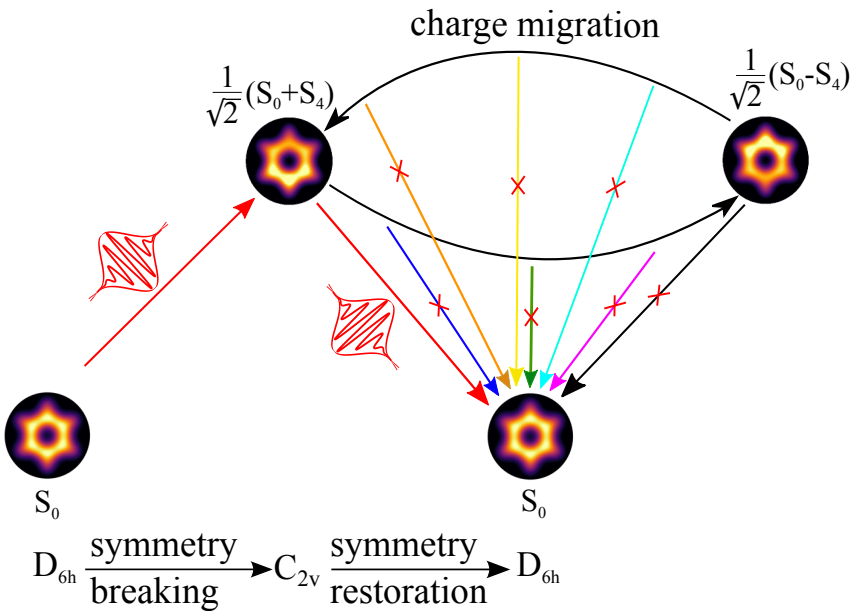

Figure 5.2: Coherent control symmetry breaking and restoration of electronic structure by means of two time-reversed copy of linearly polarized ultrashort intense laser pulses (schematic). The figure is adapted from **Paper** SR2.

Strategy 2 in **Paper** SR2 is presented with two scenarios: in the first scenario, time-reversed non-

chirped ultrashort intensive linearly y-polarized pulses with Gaussian shapes are employed; in the second scenario, time-reversed ultrashort intense down- and up-chirps are used. Two pulses are well separated and the central time is in a field-free environment, during the moment the populations of the ground and excited state are constant with irrespective of a phase factor. The snapshots of one-electron density visualize the process of symmetry breaking, charge migration and symmetry restoration. The target excited state is the only state that can be reached from the ground state by one-photon transition. The phase difference sensitively depends on the time delay between the peaks of two pulses. In principle, phase conditions should be satisfied exactly, but in practice, little less accurate may also be acceptable. Therefore, for successful symmetry restoration, one has to adjust the time delay carefully such that the phase difference is 0 or $\pm\pi$. The numerical results for linearly and chirped pulses yield great agreement with the analytical prediction. Each pair of the time evolution of the population shows multiple wiggles, which are associated with the down- and up-chirp pulses. **Paper** SR2 presents a new challenge and opportunities in the field of attosecond coherent control of electronic symmetry breaking and restoration by means of ultrashort intense laser pulses. This also improves our fundamental understanding of attosecond science and adds to the arsenal of methods in the field of quantum control.

For understanding the symmetry restoration process deeper, in **Paper** SR3 we design a new Strategy 3 to control the symmetry breaking and restoration in excited states of benzene. It develops a general strategy of electronic symmetry restoration, which shows that the laser pulses for symmetry breaking and restoration can be designed in a more general way with less severe restrictions. Our target excited state is same as in **Paper** SR1. But this new strategy gets rid of the restrictions that the two pulses for symmetry breaking and restoration must be identical in SR1, and time-reversed copy of each other in SR2. The first pulse for symmetry breaking can be arbitrary and the second pulse will be tailored to restore the symmetry in excited state. Since the laser carrier frequencies are much longer than the molecular size corresponding to the wavelengths, therefore, the electric fields are homogeneous in the molecular time domain we are interested in. The electronic ground state has D_{6h} symmetry with $IRREP = A_{1g}$, and the excited state also has D_{6h} symmetry but with a different $IRREP = E_{1u}$. We find that the pure electronic excited state belongs to the same symmetry point group as the ground state, which implies that it is also possible to restore the symmetry by creating a pure excited state.

We also know that for creating a pure excited state from the ground state by two pulses, totally a resonant π-pulse is required, which denoting that $\epsilon_e\tau_b + \epsilon_r\tau_r = \epsilon_\pi\tau_\pi$, irrespective of the polarization of the laser pulses, e.g. they can be linearly or circularly polarized pulses. Here, $\epsilon_e, \epsilon_r, \epsilon_\pi$ and τ_b, τ_r, τ_π are the amplitude of electric field and the pulse duration for the first, second and π-pulse, respectively.

Each of the pulse for symmetry breaking and restoration can be considered as a fractional π-pulse. For example, we can set the first pulse as a reference, and set the second pulse with same shape and duration, then the amplitude of the second pulse ϵ_r can be obtained by filling the gap between ϵ_b and ϵ_π.

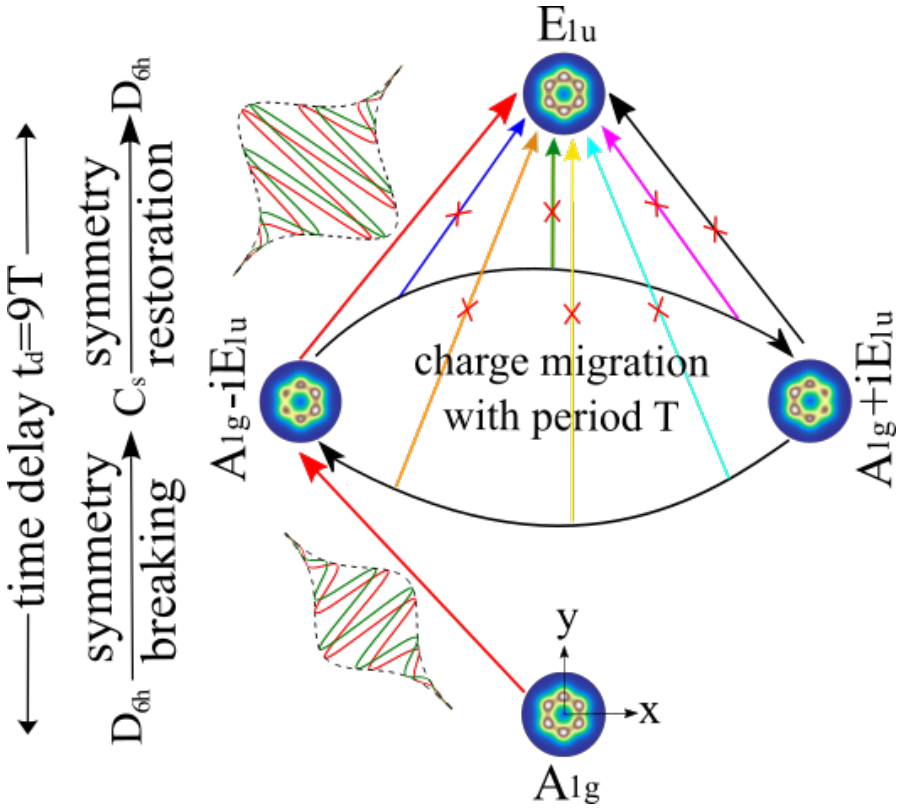

Figure 5.3: Coherent control symmetry restoration in excited state. (**Bottom**) One-electron density of the ground state labeled A_{1g}. (**Middle**) Periodic charge migration from "$A_{1g} - iE_{1u}$" via "$A_{1g} + iE_{1u}$" back to "$A_{1g} - iE_{1u}$", with period $T = 504$ as. (**Top**) One-electron density of the excited target state labeled E_{1u}. These depictions are adapted from **Paper** SR3.

In Fig. 5.3, the electronic ground state of oriented benzene molecule is labeled as A_{1g} (with symmetry D_{6h}). In order to achieve the symmetry restoration in excited state, the first circularly polarized pulse is centered at $t_b = -4.5T$. It breaks symmetry by exciting the electronic ground state to the superposition (labeled "$A_{1g} - iE_{1u}$") of the ground and the excited state. This laser excitation process is symbolized by the first red arrow (lower one). The superposition state has symmetry C_s at any time . The charge migration between the two degenerate superposition states is symbolized by the two black curved arrows, with snapshots of the one-electron density for state "$A_{1g} - iE_{1u}$" (left) at time $t = 0, T, 2T, ..$ and for state "$A_{1g} + iE_{1u}$" (right) at time $t = T/2, 3T/2, 5T/2....$ The second laser pulse centered at $t_r = 4.5T$ restores D_{6h} symmetry by transferring the superposition state completely to the pure excited state with $IRREP = E_{1u}$. This laser excitation is symbolized by the second red arrow. The different IRREPs of the electronic ground (A_{1g}) and excited state (e_{1u}) leads a very little difference

of the one-electron density for ground and excited state shown in Fig. 5.3. The bandwidths of the laser pulses may cover few energy levels with different IRREPs, whereas our target excited state is the only one that have the specific IRREP according to the symmetry selection rule.

For successful symmetry restoration in excited state of benzene, the time delay between the peaks of the laser pulses must be equal to an integer number of charge migration period, such that the phase difference at the central time is $\pm\frac{\pi}{2}$. All other crossed color arrows in Fig. 5.3 corresponding to incomplete cycles of charge migration period are failed cases of restoring the symmetry in excited state. The new methodology shows the successful quantum control symmetry breaking in the ground state with $IRREP = A_{1g}$ but symmetry restoration in the excited state with a different $IRREP = E_{1u}$.

Strategy 4 in **Paper** SR4 denotes a special case of 50% excitation from the electronic ground state of benzene to an excited state ($IRREP = A_{1g}$) by a right-circularly polarized pulse, which documents a circular attosecond charge migration. The numerical findings indicate that one can restore the symmetry either in the electronic ground state with the same IRREP when the phase difference is 0 or $\pm\pi$, or restore the symmetry in the excited state with a different IRREP when the phase difference is $\pm\frac{\pi}{2}$. Each pulse is a $\frac{\pi}{2}$-pulse. The phase difference depends sensitively on the time delay in few attoseconds. When the time delay $t_d = \left(N + \frac{1}{2}\right) T$, the second pulse de-excites the superposition state back to the electronic ground state, and restore the symmetry in ground state as in **Paper** SR1. Otherwise, when the time delay $t_d = NT$, the second pulse excites the superposition state further completely to the pure excited state, namely stop the attosecond charge migration and restore the symmetry in excited state as in **Paper** SR3. For this case, the second pulse serves either as a pump or dump pulse, depending on phase difference, which depends on the time delay in few attoseconds precision. It implies that we can restore the symmetry twice per period when two pulses are $\frac{\pi}{2}$-pulse.

The analytical formula of the final population of the excited state in **Paper** SR4 serves as a bridge between **Paper** SR1, SR2 and SR3. The two laser pulses for symmetry breaking and restoration in **Paper** SR1, SR2 and SR4 are either identical or time reversed copy of each other, e.g. with the same Gaussian shape, same carrier frequencies, same maximum field strengths etc. But in **Paper** SR3, these two laser pulses are arbitrary as long as the net effect of these two laser pulses can be summarized to be a complete excitation from the ground state to a pure excited state with a different IRREP, which implies that the sum of the two laser pulses must be a π-pulse and each pulse can be considered as a fractional π-pulse.

Paper SR1 - SR4 document a new physical phenomenon of electronic symmetry breaking and restoration in atoms and molecules, together with four new strategies for the control. The results of the publications that are shown up in this dissertation demonstrate that the laser pulse can not

Table 5.1: Comparison of four different strategies for laser control of electronic structure symmetry restoration

paper	**SR1**	**SR2**	**SR3**	**SR4**
pulse	circularly	linearly, chirp	circularly	circularly
excitation	0.37%	50%	30%	50%
time delay	$t_d = \left(N + \frac{1}{2}\right) T$	—	$t_d = NT$	$t_d = \left(N + \frac{1}{2}\right) T$ or NT
phase difference	$\{0, \pm\pi\}$	$\{0, \pm\pi\}$	$\left\{-\frac{\pi}{2}, +\frac{\pi}{2}\right\}$	$\{0, \pm\pi\}$ or $\left\{-\frac{\pi}{2}, +\frac{\pi}{2}\right\}$
population	$4P_g(t_c)P_e(t_c)\left[1 - \cos\left(\frac{2\pi t}{t}\right)\right]$		$1 - 2P_g(t_c)P_e(t_c)\left[1 - \cos\left(\frac{2\pi t}{T}\right)\right]$	
symmetry restoration	ground state	ground state	excited state	ground or excited state

only break the symmetry, but also can restore the symmetry. The four strategies described above offer us a choice to restore the symmetry either in the ground state or in an excited state coherent controlled by well-designed ultrashort laser pulses. The success depends on the Hamiltonian condition and the associated phase conditions, which depend on the time delay between the peaks of two pulses in few attoseconds precision. All important information of the four strategies are listed in **Table** 5.1.

In the first part of this dissertation, we give a discussion of attosecond coherent control of symmetry restoration in atoms and molecules using semiclassical formulism. In particular, we give an essentially numerical analysis of the population of excited state driven by two time-delayed ultrashort pulses and study the influence of the time delay on the phase difference. The first pulse creates a superposition state, while the second time-delayed pulse can either de-excite the superposition back to the ground state, which is associated with symmetry restoration in ground state with same IRREP; or excite the superposition further to a pure excited state, which is associated with symmetry restoration in excited state with a different IRREP. For a time delay equals half time the charge migration period, the second pulse will de-excite the superposition back to the ground state. For a time delay equals an integer number of the charge migration period, the second pulse excites the superposition state created by the first pulse further more to the excited state. The phase difference is extremely sensitive of the time delay between two pulses. The total population of the excited state after the pulse sequence is modulated by the time delay. Our work show that careful manipulation of the phase conditions can be used to trace and control the ultrafast attosecond process in atoms and molecules. We present a controlled switching of symmetry from highly symmetric electronic ground state to a less symmetric

superposition and back to a highly symmetric pure state by sequence time-delayed pulses.

In conclusion, the general procedure for quantum control symmetry breaking and restoration in excited state contains three steps:

(1) symmetry breaking by the first laser pulse;

(2) ultrafast attosecond charge migration, and determine phase difference;

(3) design the second laser pulse for symmetry restoration.

This work may have a fascinating effect to attosecond science.[8–10, 22, 24] The remaining of this dissertation will thus focus on this very important aspect of attosecond chemistry. This methodological framework is then applied for quantitative investigations of attosecond charge migration processes in different superposition states of the oriented benzene molecule. Charge migration plays an important role in symmetry restoration, as it determines the phase of the electronic wave function around the central time.

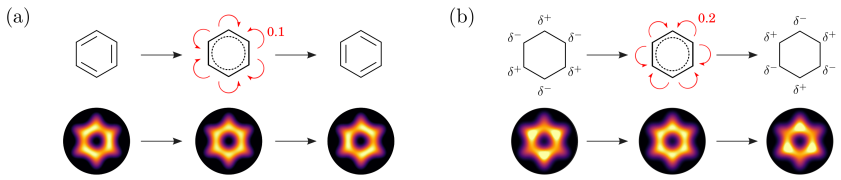

Figure 5.4: Mechanism of ultrafast attosecond charge migration in different superposition states of benzene molecule. Upper panels of (a) and (b) show the Lewis structures of the two superposition states. Lower panels of (a) and (b) show the time evolution of the one-electron density for associated superposition states. The red arrows refer the charge migration directions corresponding to two different mechanisms. This figure is adapted from **Paper** CM1 and CM2.

As we mentioned earlier, laser control aromaticity of benzene molecule by Ulusoy and Nest[49] is proved to be our inspiration to laser control symmetry of electronic structure in atoms and molecules. They prepared two non-aromatic superposition states $S_0 + S_1$ (called Kekulé structures together with degenerate superposition $S_0 - S_1$, see upper panels of Fig. 5.4a) and $S_0 + S_2$ by exciting the molecule from its aromatic electronic ground state S_0 to the first and second non-aromatic singlet excited states S_1 (with $IRREP = B_{2u}$ in D_{6h} symmetry point group) and S_2 (with $IRREP = B_{1u}$ in D_{6h} symmetry point group). The aromaticity of benzene molecule was measured by the corresponding bond orders and Mulliken charges. They demonstrated that the electron charge are localized on bonds for superposition $S_0 + S_1$ and partial positive and negative charges on alternating carbon atoms for $S_0 + S_2$. The localized electrons circulate in the ring system in attosecond time scale, where the nuclei are essentially frozen, thus the effects of kinetic couplings (non-adiabatic couplings) are negligible. Therefore, both processes correspond to adiabatic attosecond charge migration (AACM) processes. They estimated that totally 4.2 electrons are moving in the ring system for $S_0 + S_1$ and 1.5 electrons

participate for $S_0 + S_2$. They also estimated that the electron charge moves in a pincer motion between two equivalent Kekulé structures but without giving any quantitative analysis.

Therefore, for finding out how the electrons really move during the AACM, in **Paper** CM1 and CM2, we focus on the quantitative analysis of electronic flux density during AACM for two non-aromatic superpositions of the oriented benzene molecule. In CM1, we prepare the non-aromatic superposition by 50% exciting the aromatic electronic ground state to the first non-aromatic singlet excited state, which initiates AACM between two equivalent Kekulé structures. The simulation results indicate that the electron charges are localized on every two bonds and the angular electronic flux during the AACM presents a pincer-type motion with "sources" and "sinks" at the center of alternating bonds varies periodically with $T = 848\ as$, which depend on the energy difference between the ground state S_0 and excited state S_1. The ground and first excited state are based on CASSCF(6,12) calculations for the wave functions and CI singles and doubles calculations for the energies of excited states with cc-pVTZ basis set.

The theory for angular electronic fluxes during the AACM for a ring-shaped molecule is transfered from the previous theory on coherent tunneling[97] and the electronic continuity equation is used with a problem specific boundary condition to analyze the angular electronic fluxes. Due to the computational costs, total wave function is represented by few selected dominant Slater determinants and all others that contribute less than one percent are neglected. The angular electronic flux indicates that the charge migration is pincer-type pattern. The integration of the angular electronic density difference yields maximum 0.48 electrons flow concertedly through half the molecule plane. The error ± 0.02 is estimated qualitatively, because only few dominant Slater determinants are taken into account for the wave function calculation. The error is specific for our choice of basis set and method. This amounts to about 25% error due to the small number of electrons involved in the charge migration, however, this does not affect the subsequent conclusions. The theory in **Paper** CM1 presents the first application of the charge migration in an excited superposition state of oriented benzene molecule. The results confirm the hypothesis of ref. [49] that the AACM in $S_0 + S_1$ is pincer-type motion, but the number of the electrons that transferred during the AACM process is much smaller than their estimation of 4.2 electrons. Such a small amount of electrons flow during the Kekulé structures implies that the electrons are delocalized on the system, e.g. most electrons that are assigned to double bonds in Kekulé structures actually penetrate into the neighboring single bonds. Consequently, large fraction of electrons do not need to move. This phenomenon has been noted for electronic fluxes during molecular reactions and vibrations in the electronic ground states (see ref. [118–123]) that the effect of delocalization of electrons resulting in very small fraction of moving electrons. In principle, the Full

CI calculation will give an exact number of electrons that flow during the process for a given basis.

Paper CM2 generates a non-aromatic superposition $S_0 + S_2$ of the aromatic electronic ground and the second nonaromatic singlet excited state, where negative and positive charges are spatially localized on alternating carbon nuclei. The quantum chemistry calculation is done in CASSCF(6,6) level, aug-cc-pVTZ basis set and the energy calculation at MRCISD level.

The wave functions are expanded in terms of all 104 Slater determinants in the frame of CASSCF(6,6) method, which give us more accurate results. For our specific choice of the polarization of the pulses and the molecular geometry, the electronic flux is equal to zero in yz-symmetry plane, which also implies that the electrons never move across any nucleus. The "sources" and "sinks" of electrons are on alternating carbon nuclei while the electronic density flux flow between the nuclei but never across the nuclei, which is contrast to the findings of **Paper** CM1 that the electrons flow across the carbon nuclei from bonds to bonds. The "sources" and "sinks" interchange clockwise and anticlockwise during the first half period and reverse directions during the second half period, with period $T = 590\ as$, see lower panel of Fig. 5.4b. The electrons flow away from three alternating carbon nuclei with surplus of electronic density δ^- towards three neighboring carbon nuclei with a deficit of electronic density δ^+. The integration of electronic density difference over all but one coordinate gives us the direction of the electronic density flux, which shows a pincer-type motion. The total number of electrons flow concertedly clockwise or anti-clockwise involved in the charge migration process is $6 \times 0.2 = 1.2$.

Based on this improved method and basis set, we find that the results (angular electronic density difference, yield and electronic density flux) for taking all 104 Slater determinants or only few dominant Slater determinants into account show good agreement for superposition $S_0 + S_2$, but identical for superposition $S_0 + S_1$. This indicates that the properties of the angular electronic fluxes in non-aromatic superposition states of benzene molecule are determined by very few dominant Slater determinants for representing the wave functions of the electronic ground and two lowest-lying excited singlet states that involved in these two cases. The better method and basis give a more accurate number of electrons that participate during AACM of $S_0 + S_1$, namely 0.72 electrons for CASSCF(6,6) and basis aug-cc-pVTZ with MRCISD energy calculations, with comparison with 0.48 electrons for CASSCF(6,12) and basis cc-pVTZ calculation, 30% improved. For the current method and basis choice, the total number of electrons (1.2 electrons) flow in $S_0 + S_2$ is almost twice as large as 0.72 electrons flow in $S_0 + S_1$.

In **Paper** CM1 and CM2, we determine the angular electronic density flux during AACM in two different non-aromatic superposition states of oriented benzene molecule and specify the number of electrons that participate in the charge migration process. Besides the different charge migration

periods and the number of electrons participated in AACM, the mechanistic difference between these two cases is that the "sinks" and "sources" of the electronic angular fluxes are at alternating bond centers for $S_0 + S_1$ and at alternating carbon nuclei for $S_0 + S_2$, but the maximum of the flux are at the carbon nuclei and at the CC bond centers, respectively. Control of the ultrafast attosecond charge migration process echo our work in **Paper** SR1 - SR4 of coherent control electronic structure symmetry breaking and restoration in attosecond time scale and few attoseconds precision.

The following context serves as a brief outlook. In our present theory of symmetry restoration in molecule, we did not consider molecular vibrations, which play a role at longer times. However, the proof-of-principle we propose here should remain valid when including vibrational motion, but it will be more difficult. One simple extension of current model is the coupled electron-vibration dynamics along the Jahn-Teller coordinates, which causes a further loss of symmetry and will affect charge migration. The associated dynamics will also be more complicated. The chemical reactivity of BH_3 molecule can also be potentially controlled by exciting the molecule to molecular vibrational excited state and then de-excites the molecule back to the ground nuclear configuration to restore the symmetry. The molecular chirality controlled by laser pulse can be another extension application. The theory may also attractive for intermolecular interactions in dense gases, and vibrational relaxation. The present theory for coherent control of symmetry breaking and restoration of electronic structure can be expanded to multi-photon excitation symmetry restoration and offer an exciting new frontier for attosecond science.

The theory in CM1 and CM2 allows to prepare analogous initial state for other ring-shaped or linear molecules and also to create the initial state in a large variety of different superpositions of electronic states. The general theory of electronic flux during AACM in ring-shaped molecules supports many kinds of applications, e.g. prepare oriented benzene molecule in an arbitrarily large variety of different superposition states. The theory predicts that different initial superpositions of eigenstates induce different flux patterns and will induce significant variations of the flux patterns when more excited tunneling doublets are prepared.

Bibliography

[1] T. D. Lee and C. N. Yang, "Question of parity conservation in weak interactions", Phys. Rev. **104**, 254–258 (1956) (cit. on p. 1).

[2] M. Quack, "On biomolecular homochirality as a quasi-fossil of the evolution of life", Adv. Chem. Phys. **157**, 249–290 (2014) (cit. on p. 1).

[3] N. S. M. Borštnik, "Can spin-charge-family theory explain baryon number nonconservation?", Phys. Rev. D **91**, 065004 (2015) (cit. on p. 1).

[4] D. Tannor, *Introduction to quantum mechanics: a time-dependent perspective* (University Science Books, Sausalito, Calif, 2007) (cit. on pp. 1, 7–9, 11, 13, 15, 17, 30).

[5] H. W. Kroto, J. R. Heath, S. C. O'Brien, R. F. Curl, and R. E. C. Smalley, "C_{60}: Buckminsterfullerene", Nature **318**, 162–163 (1985) (cit. on p. 1).

[6] P. B. Corkum, "Plasma perspective on strong-field multiphoton ionization", Phys. Rev. Lett. **71**, 1994–1997 (1993) (cit. on p. 1).

[7] P. B. Corkum and F. Krausz, "Attosecond science", Nat. Phys. **3**, 381–387 (2007) (cit. on pp. 1, 4).

[8] F. Krausz and M. Ivanov, "Attosecond physics", Rev. Mod. Phys. **81**, 163–234 (2009) (cit. on pp. 1, 2, 4, 168).

[9] S. Chelkowski, T. Bredtmann, and A. D. Bandrauk, "High-order-harmonic generation from coherent electron wave packets in atoms and molecules as a tool for monitoring attosecond electrons", Phys. Rev. A **85**, 033404 (2012) (cit. on pp. 1, 168).

[10] T. Schultz and M. Vrakking, *Attosecond and XUV physics* (Wiley-VCH: Weinheim, Germany, 2014) (cit. on pp. 1, 168).

[11] G. Alber, H. Ritsch, and P. Zoller, "Generation and detection of Rydberg wave packets by short laser pulses", Phys. Rev. A **34**, 1058–1064 (1986) (cit. on p. 2).

[12] L. D. Noordam, D. I. Duncam, and T. F. Gallagher, "Ramsey fringes in atomic Rydberg wave packets", Phys. Rev. A. **45**, 4734–4737 (1992) (cit. on p. 2).

[13] Y. Arasaki and K. Takatsuka, "Optical conversion of conical intersection to avoided crossing", Phys. Chem. Chem. Phys. **120**, 1239–1242 (2010) (cit. on p. 2).

[14] W. P. Schleich and H. Walther(Eds.), *Elements of quantum information* (Wiley-VCH, Weinheim, 2007) (cit. on p. 2).

[15] J. Parker and C. R. S. Jr., "Coherence and decay of Rydberg wave packets", Phys. Rev. Lett. **56**, 716–719 (1986) (cit. on p. 2).

[16] M. Ivanov, P. B. Corkum, and P. Dietrich, "Coherent control and collapse of symmetry in a two-level system in an intense laser field", Laser Phys. **3**, 375–380 (1993) (cit. on p. 2).

[17] T. C. Weinacht, J. Ahn, and P. H. Bucksbaum, "Measurement of the amplitude and phase of a sculpted Rydberg wave packet", Phys. Rev. Lett. **80**, 5508–5011 (1998) (cit. on p. 2).

[18] N. Elghobashi, L. González, and J. Manz, "Quantum model simulations of symmetry breaking and control of bond selective dissociation of FHF^- using IR+UV laser pulses", J. Chem. Phys. **120**, 8002 (2004) (cit. on p. 2).

[19] H. Maeda, D. V. L. Norum, and T. F. Gallagher, "Microwave manipulation of an atomic electron in a classical orbit", Science **307**, 1757–1760 (2005) (cit. on p. 2).

[20] I. Barth and J. Manz, "Periodic electron circulation induced by circularly polarized laser pulses: quantum model simulations for Mg Porphyrin", Angew. Chem. Int. Ed. **45**, 2962–2965 (2006) (cit. on pp. 2, 4, 5).

[21] Y. Arasaki, K. Wang, V. McKoy, and K. Takatsuka, "Monitoring the effect of a control pulse on a conical intersection by time-resolved photoelectron spectroscopy", Phys. Chem. Chem. Phys. **13**, 8681–8689 (2011) (cit. on p. 2).

[22] A. S. Alnasser, M. Kübel, R. Siemering, B. Bergues, N. G. Kling, K. J. Betsch, Y. Deng, J. Schmidt, Z. A. Alahmed, A. M. Azzeer, J. Ullrich, I. Ben-Itzhak, R. Moshammer, U. Kleineberg, F. Krausz, R. de Vivie-Riedle, and M. F. Kling, "Subfemtosecond steering of hydrocarbon deprotonation through superposition of vibrational modes", Nature Commun. **5**, 3800 (2014) (cit. on pp. 2, 168).

[23] M. N. Daud, H. Lu, S. Chelkowski, and A. D. Bandrauk, "Quantum control of electron-proton symmetry breaking in dissociative ionization of H_2 by intense laser pulses", Int. J. Quant. Chem. **115**, 369–380 (2015) (cit. on pp. 2, 4).

[24] Y. Pertot, C. Schmidt, M. Matthews, A. Chauvet, M. Huppert, V. Svoboda, A. Conta, A. Tehlar, D. Baykusheva, J.-P. Wolf, and H. J. Wörner, "Time-resolved X-ray absorption spectroscopy with a water window high-harmonic source", Science **355**, 264–267 (2017) (cit. on pp. 2, 168).

[25] L. S. Cederbaum and J. Zobeley, "Ultrafast charge migration by electron correlation", Chem. Phys. Lett. **307**, 205–210 (1999) (cit. on pp. 2, 4).

[26] F. Remacle and R. D. Levine, "An electronic time scale in chemistry", Proc. Natl. Acad. Sci. USA **103**, 6793–6798 (2006) (cit. on pp. 2, 4, 5).

[27] S. Chelkowski, G. L. Yudin, and A. D. Bandrauk, "Observing electron motion in molecules", J. Phys. B **39**, S409–S417 (2006) (cit. on pp. 2, 4).

[28] M. Kanno, H. Kono, and Y. Fujimura, "Control of π-electron rotation in chiral aromatic molecules by nonhelical laser pulses", Angew. Chem. Int. Ed. **45**, 7995–7998 (2006) (cit. on pp. 2, 4).

[29] H. Mineo, S. H. Lin, and Y. Fujimura, "Vibrational effects on UV/Vis laser-driven π-electron ring currents in aromatic ring molecules", Chem. Phys. **442**, 103–110 (2014) (cit. on pp. 2, 4).

[30] V. Despré, A. Marciniak, V. Loriot, M. C. E. Galbraith, A. Rouzée, M. J. J. Vrakking, F. Lépine, and A. I. Kuleff, "Attosecond hole migration in benzene molecules surviving nuclear motion", J. Phys. Chem. Lett. **6**, 426–431 (2015) (cit. on pp. 2, 4).

[31] P. M. Kraus, B. Mignolet, D. Baykusheva, A. Rupenyan, L. Horny, E. F. Penka, G. Grassi, O. I. Tolstikhin, J. Schneider, and F. Jensen, "Measurement and laser control of attosecond charge migration in ionized iodoacetylene", Science **350**, 790–795 (2015) (cit. on pp. 2, 4, 5).

[32] K. Ueda, "To catch and smash charge on the hop", Science **350**, 740–741 (2015) (cit. on p. 2).

[33] D. Jia, J. Manz, B. Paulus, V. Pohl, J. C. Tremblay, and Y. Yang, "Quantum control of electronic fluxes during adiabatic attosecond charge migration in degenerate superposition states of benzene", Chem. Phys. **482**, 146 (2017) (cit. on p. 2).

[34] N. V. Golubev, V. Despré, and A. Kuleff, "Quantum control with smoothly varying pulses: general theory and application to charge migration", J. Mod. Opt. **64**, 1031–1041 (2017) (cit. on p. 2).

[35] D. J. Tannor and S. A. Rice, "Control of selectivity of chemical reaction via control of wave packet evolution", J. Chem. Phys. **83**, 5013 (1985) (cit. on p. 2).

[36] C. Brif, R. Chakrabarti, and H. Rabitz, "Control of quantum phenomena: past, present and future", New J. Phys. **12**, 075008 (2010) (cit. on p. 2).

[37] M. Shapiro and P. Brumer, *Quantum control of molecular processes, 2nd ed.* (WILEY-VCH, Weinheim, 2012) (cit. on p. 2).

[38] H. J. Wörner, C. A. Arrell, N. Banerji, A. Cannizzo, M. Chergui, A. K. Das, P. Hamm, U. Keller, P. M. Kraus, E. Liberatore, P. Lopez-Tarifa, M. Lucchini, M. Meuwly, C. Milne, J.-E. Moser, U. Rothlisberger, G. Smolentsev, J. Teuscher, J. A. van Bokhoven, and O. Wenger, "Charge migration and charge transfer in molecular systems", Struct. Dyn. **4**, 061508 (2017) (cit. on pp. 2, 4).

[39] E. E. B. Campbell, H. Schmidt, and I. V. Hertel, "Symmetry and angular momentum in collisions with laser excited polarized atoms", Adv. Chem. Phys. **72**, 37–114 (1998) (cit. on p. 2).

[40] E. Halevi, *Orbital symmetry and reaction mechanism: the ocams view* (Springer: Berlin, Germany, 1992) (cit. on p. 2).

[41] S. Al-Jabour and M. Leibscher, "Effects of molecular symmetry on quantum reaction dynamics: novel aspects of photoinduced nonadiabatic dynamics", J. Phys. Chem. A **119**, 271–280 (2015) (cit. on p. 2).

[42] I. Barth and J. Manz, *Progress in ultrafast intense laser science VI* (Springer, Berlin, 2010) (cit. on p. 2).

[43] J. M. N. Djiokap, S. X. Hu, L. B. Madsen, N. L. Manakov, A. V. Meremianin, and A. F. Starace, "Electron vortices in photoionization by circularly polarized attosecond pulses", Phys. Rev. Lett. **115**, 113004 (2015) (cit. on p. 2).

[44] F. Mauger, A. D. Bandrauk, and T. Uzer, "Circularly polarized molecular high harmonic generation using a bicircular laser", J. Phys. B: At. Mol. Opt. Phys. **49**, 10LT01 (2016) (cit. on p. 2).

[45] X. Liu, X. Zhu, L. Li, Y. Li, Q. Zhang, P. Lan, and P. Lu, "Selection rules of high-order-harmonic generation: symmetries of molecules and laser fields", Phys. Rev. A **94**, 033410 (2016) (cit. on p. 2).

[46] K.-J. Yuan and A. D. Bandrauk, "Symmetry in circularly polarized molecular high-order harmonic generation with intense bicircular laser pulses", Phys. Rev. A **97**, 023408 (2018) (cit. on p. 2).

[47] D. Baykusheva, M. S. Ahsan, N. Lin, and H. J. Wörner, "Bicircular high-harmonic spectroscopy reveals dynamical symmetries of atoms and molecules", Phys. Rev. Lett. **116**, 123001 (2016) (cit. on p. 2).

[48] J. Köhler, M. Wollenhaupt, T. Bayer, C. Sarpe, and T. Baumert, "Zeptosecond precision pulse shaping", Opt. Exp. **9**, 11638–11653 (2011) (cit. on p. 3).

[49] I. Ulusoy and M. Nest, "Correlated electron dynamics: how aromaticity can be controlled?", J. Am. Chem. Soc. **133**, 20230–20236 (2011) (cit. on pp. 3–5, 157, 168, 170).

[50] A. Marian, M. C. Stowe, J. R. Lawall, D. Felinto, and J. Ye, "United time-frequency spectroscopy for dynamics and global structure", Science **306**, 2063 (2004) (cit. on p. 3).

[51] D. Tong, S. M. Farooqi, J. Stanojevic, S. Krishnan, Y. P. Zhang, R. Côté, E. E. Eyler, and P. L. Gould, "Local blockade of Rydberg excitation in an ultracold gas", Phys. Rev. Lett. **93**, 063001 (2004) (cit. on p. 3).

[52] K. Singer, M. Reetz-Lamour, T. Amthor, L. Marcassa, and M. Weidemüller, "Suppression of excitation and spectral broadening induced by interactions in a cold gas of Rydberg atoms", Phys. Rev. Lett. **93**, 063001 (2004) (cit. on p. 3).

[53] N. Takei, C. Sommer, C. Genes, G. Pupillo, H. Goto, K. Koyasu, H. Chiba, M. Weidemüller, and K. Ohmori, "Direct observation of ultrafast many-body electron dynamics in an ultracold Rydberg gas", Nature Commun. **7**, 13449 (2016) (cit. on p. 3).

[54] J. Wolters, G. Buser, A. Horsley, L. Béguin, A. Jöckel, J.-P. Jahn, R. J. Warburton, and P. Treutlein, "Simple atomic quantum memory suitable for semiconductor quantum dot single photons", Phys. Rev. Lett. **119**, 060502 (2017) (cit. on p. 3).

[55] H. Eyring, J. Walter, and G. E. Kimball, *Quantum chemistry* (Wiley, New York, 1944), pp. 198–200 (cit. on p. 4).

[56] R. Weinkauf, P. Schanen, D. Yang, S. Soukara, and E. W. Schlag, "Elementary processes in peptides: electron mobility and dissociation in peptide cations in the gas phase", J. Phys. Chem. **99**, 11255–11265 (1995) (cit. on p. 4).

[57] R. Weinkauf, P. Schanen, A. Metsala, E. W. Schlag, M. Bürgle, and H. Kessler, "Highly efficient charge transfer in peptide cations in the gas phase: threshold effects and mechanism", J. Phys. Chem. **100**, 18567–18585 (1996) (cit. on pp. 4, 5).

[58] R. Weinkauf, E. W. Schlag, T. J. Martinez, and R. D. Levine, "Nonstationary electronic states and site-selective reactivity", J. Phys. Chem. A **101**, 7702–7710 (1997) (cit. on p. 4).

[59] E. W. Schlag, H. L. Selzle, P. Schanen, R. Weinkauf, and R. D. Levine, "Dissociation kinetics of peptide ions", J. Phys. Chem. A **110**, 8494–8500 (2006) (cit. on p. 4).

[60] F. Remacle, R. Levine, and M. Ratner, "Charge directed reactivity: a simple electronic model, exhibiting site selectivity, for the dissociation of ions", Chem. Phys. Lett. **285**, 25–33 (1998) (cit. on p. 4).

[61] B. Mignolet, R. D. Levine, and F. Remacle, "Charge migration in the bifunctional PENNA cation induced and probed by ultrafast ionization: a dynamical study", J. Phys. B: At. Mol. Opt. Phys. **47**, 124011 (2014) (cit. on p. 4).

[62] J. Breidbach and L. S. Cederbaum, "Migration of holes: formalism, mechanisms, and illustrative applications", J. Chem. Phys. **118**, 3983–3996 (2003) (cit. on p. 4).

[63] H. Hennig, J. Breidbach, and L. S. Cederbaum, "Electron correlation as the driving force for charge transfer: charge migration following ionization in *n*-methyl acetamide", J. Phys. Chem. A **109**, 409–414 (2005) (cit. on p. 4).

[64] S. Lünnemann, A. I. Kuleff, and L. S. Cederbaum, "Ultrafast charge migration in 2-phenylethyl-N, *n*-dimethylamine", Chem. Phys. Lett. **450**, 232–235 (2008) (cit. on p. 4).

[65] A. I. Kuleff, S. Lünnemann, and L. S. Cederbaum, "Electron-correlation-driven charge migration in oligopeptides", Chem. Phys. **414**, 100–105 (2013) (cit. on p. 4).

[66] A. I. Kuleff and L. S. Cederbaum, "Ultrafast correlation-driven electron dynamics", J. Phys. B: At., Mol. Opt. Phys. **47**, 124002 (2014) (cit. on p. 4).

[67] A. I. Kuleff, N. V. Kryzhevoi, M. Pernpointner, and L. S. Cederbaum, "Core ionization initiates subfemtosecond charge migration in the valence shell of molecules", Phys. Rev. Lett. **117**, 093002 (2016) (cit. on p. 4).

[68] G. L. Yudin, S. Chelkowski, J. Itatani, A. D. Bandrauk, and P. B. Corkum, "Attosecond photoionization of coherently coupled electronic states", Phys. Rev. A **72**, 051401 (2005) (cit. on p. 4).

[69] A. D. Bandrauk, S. Chelkowski, P. B. Corkum, J. Manz, and G. L. Yudin, "Attosecond photoionization of a coherent superposition of bound and dissociative molecular states: effect of nuclear motion", J. Phys. B: At. Mol. Opt. Phys. **42**, 134001 (2009) (cit. on p. 4).

[70] H. Mineo, S. H. Lin, and Y. Fujimura, "Coherent π-electron dynamics of (p)-2, 2'-biphenol induced by ultrashort linearly polarized UV pulses: angular momentum and ring current", J. Chem. Phys. **138**, 074304 (2013) (cit. on p. 4).

[71] M. F. Kling, P. von den Hoff, I. Znakovskaya, and R. de Vivie-Riedle, "(sub-)femtosecond control of molecular reactions via tailoring the electric field of light", Phys. Chem. Chem. Phys. **15**, 9448–9467 (2013) (cit. on p. 4).

[72] F. Calegari, D. Ayuso, A. Trabattoni, L. Belshaw, S. D. Camillis, S. Anumula, F. Frassetto, L. Poletto, A. Palacios, P. Decleva, J. B. Greenwood, F. Martin, and M. Nisoli, "Ultrafast electron dynamics in phenylalanine initiated by attosecond pulses", Science **346**, 336–339 (2014) (cit. on p. 4).

[73] H. Ding, D. Jia, J. Manz, and Y. Yang, "Reconstruction of the electronic flux during adiabatic attosecond charge migration in $HCCI^+$", Molec. Phys. **115**, 1813–1825 (2017) (cit. on p. 4).

[74] J. M. D. J. Diestler G. Hermann, "Charge migration in Eyring, Walter and Kimball's 1944 model of the electronically excited hydrogen-molecule ion", J. Phys. Chem. A **121**, 5332–5340 (2017) (cit. on p. 4).

[75] M. Hentschel, R. Kienberger, C. Spielmann, G. A. Reider, N. Milosevic, T. Brabec, P. B. Corkum, U. Heinzmann, M. Drescher, and F. Krausz, "Attosecond metrology", Nature **414**, 509–513 (2001) (cit. on p. 4).

[76] R. Kienberger, M. Hentschel, M. Uibracker, C. Spielmann, M. Kitzler, A. Scrinzi, M. Wieland, T. Westerwalbesloh, U. Kleineberg, U. Heinzmann, M. Drescher, and F. Krausz, "Steering attosecond electron wave packets with light", Science **297**, 1144–1148 (2002) (cit. on p. 4).

[77] M. Drescher, M. Hentschel, R. Kienberger, M. Uiberacker, V. Yakovlev, A. Scrinzi, T. Westerwalbesloh, U. Kleineberg, U. Heinzmann, and F. Krausz, "Time-resolved atomic inner-shell spectroscopy", Nature **419**, 803–807 (2002) (cit. on p. 4).

[78] P. H. Bucksbaum, "Attophysics: ultrafast control", Nature **421**, 593–594 (2003) (cit. on p. 4).

[79] G. G. Paulus, F. Lindner, H. Walther, A. Baltuka, E. Goulielmakis, M. Lezius, and F. Krausz, "Measurement of the phase of few-cycle laser pulses", Phys. Rev. Lett. **91**, 253004 (2003) (cit. on p. 4).

[80] J. Itatani, J. Levesque, D. Zeidler, H. Niikura, H. Pépin, J. C. Kieffer, P. B. Corkum, and D. M. Villeneuve, "Tomographic imaging of molecular orbitals", Nature **432**, 867–871 (2004) (cit. on p. 4).

[81] A. Föhlisch, P. Feulner, F. Hennies, A. Fink, D. Menzel, D. Sanchez-Portal, P. M. Echenique, and W. Wurth, "Direct observation of electron dynamics in the attosecond domain", Nature **436**, 373–376 (2005) (cit. on p. 4).

[82] M. F. Kling, C. Siedschlag, A. J. Verhoef, J. I. Khan, M. Schultze, T. Uphues, Y. Ni, M. Uiberacker, M. Drescher, F. Krausz, and M. J. J. Vrakking, "Control of electron localization in molecular dissociation", Science **312**, 246–248 (2006) (cit. on p. 4).

[83] H. J. Wörner, J. B. Bertrand, D. V. Kartashov, P. B. Corkum, and D. M. Villeneuve, "Following a chemical reaction using high-harmonic interferometry", Nature **466**, 604–607 (2010) (cit. on p. 4).

[84] B. Friedrich and D. Herschbach, "Alignment and trapping of molecules in intense laser fields", Phys. Rev. Lett. **74**, 4623C4626 (1995) (cit. on p. 5).

[85] H. Stapelfeldt and T. Seideman, "Colloquium: aligning molecules with strong laser pulses", Rev. Mod. Phys. **75**, 543–557 (2003) (cit. on p. 5).

[86] M. Leibscher, I. S. Averbukh, and H. Rabitz, "Molecular alignment by trains of short laser pulses", Phys. Rev. Lett. **90**, 213001 (2003) (cit. on p. 5).

[87] R. d. Nalda, E. Heesel, M. Lein, N. Hay, R. Velotta, E. Springate, M. Castillejo, and J. P. Marangos, "Role of orbital symmetry in high-order harmonic generation from aligned molecules", Phys. Rev. A **69**, 031804 (2004) (cit. on p. 5).

[88] S. Fleischer, I. S. Averbukh, and Y. Prior, "Selective alignment of molecular spin isomers", Phys. Rev. Lett. **99**, 093002 (2007) (cit. on p. 5).

[89] K. Oda, M. Hita, S. Minemoto, and H. Sakai, "All-optical molecular orientation", Phys. Rev. Lett. **104**, 213901 (2010) (cit. on p. 5).

[90] T. Grohmann and M. Leibscher, "Nuclear spin selective alignment of Ethylene and analogues", J. Chem. Phys. **134**, 204316 (2011) (cit. on p. 5).

[91] S. Shaik, A. Shurki, D. Danovich, and P. C. Hiberty, "Origins of the exalted B_{2u} frequency in the first excited state of benzene", J. Am. Chem. Soc. **118**, 666–671 (1996) (cit. on p. 5).

[92] A. Schild, D. Choudhary, V. D. Sambre, and B. Paulus, "Electron density dynamics in the electronic ground state: motion along the Kekulé mode of benzene", J. Phys. Chem. A **116**, 11355C11360 (2012) (cit. on p. 5).

[93] M. Okuyama and K. Takatsuka, "Electron flux in molecules induced by nuclear motion", Chem. Phys. Lett. **476**, 109–115 (2009) (cit. on p. 5).

[94] K. Nagashima and K. Takatsuka, "Electron-wavepacket reaction dynamics in proton transfer of Formamide", J. Phys. Chem. A **113**, 15240–15249 (2009) (cit. on p. 5).

[95] K. Takatsuka and T. Yonehara, "Exploring dynamical electron theory beyond the Born-Oppenheimer framework: from chemical reactivity to non-adiabatically coupled electronic and nuclear wavepackets on-the-fly under laser field", Phys. Chem. Chem. Phys. **13**, 4987–5016 (2011) (cit. on p. 5).

[96] M. Okuyama and K. Takatsuka, "Dynamical electron mechanism of double proton transfer in Formic Acid Dimer", Bull. Chem. Soc. Jpn. **85**, 217–227 (2012) (cit. on p. 5).

[97] T. Bredtmann, D. J. Diestler, S.-D. Li, J. Manz, J. F. Pérez-Torres, W.-J. Tian, Y.-B. Wu, Y. Yang, and H.-J. Zhai, "Quantum theory of concerted electronic and nuclear fluxes associated with adiabatic intramolecular processes", Phys. Chem. Chem. Phys. **17**, 29421–29464 (2015) (cit. on pp. 5, 169).

[98] A. Szabo and N. S. Ostlund, *Modern quantum chemistry: introduction to advanced electronic structure theory* (Dover Publications, New York, 1982) (cit. on pp. 7–9, 11, 13, 15, 17).

[99] E. Schrödinger, "Quantisierung als eigenwertproblem", Ann. Phys. (Leipzig) **81**, 109–139 (1926) (cit. on pp. 7, 11, 13, 15, 17).

[100] M. Born and R. Oppenheimer, "Zur quantentheorie der molekeln", Ann. Phys. (Berlin) **389**, 457C484 (1927) (cit. on pp. 8, 9).

[101] M. Born and K. Huang, *Dynamical theory of crystal lattices* (International Series of Monographs on Physics (Clarendon Press), 1954) (cit. on p. 9).

[102] W. Domcke, D. Yarkony, and H. Köppel, *Conical intersections: electronic structure, dynamics spectroscopy* (Advanced Series in Physical Chemistry (World Scientific), 2004) (cit. on p. 9).

[103] P. W. Aktins and R. S. Friedman, *Molecular quantum mechanics* (Oxford University Press, New York, 1997) (cit. on pp. 15, 19).

[104] D. Casanovaa, "Short-range density functional correlation within the restricted active space ci method", J. Chem. Phys. **148**, 124118 (2018) (cit. on p. 16).

[105] P. A. M. Dirac, "Quantum mechanics of many-electron systems", Proc. R. Soc. A **123**, 714–733 (1929) (cit. on p. 16).

[106] J. Hinze, "MC-SCF. I. The multi-configuration self-consistent-field method", J. Chem. Phys. **59**, 6424 (1973) (cit. on p. 16).

[107] D. Ma, G. L. Manni, and L. Gagliardi, "The generalized active space concept in multiconfigurational self-consistent field methods", J. Chem. Phys. **135**, 044128 (2011) (cit. on p. 16).

[108] P. A. Malmqvist, A. Rendell, and B. O. Roos, "The restricted active space self-consistent-field method, implemented with a split graph unitary group approach", J. Phys. Chem. **94**, 5477–5482 (1990) (cit. on p. 17).

[109] I. N. Levine, *Quantum chemistry* (Pearson Education, 2014) (cit. on p. 19).

[110] F. A. Cotton, *Chemical applications of group theory* (Wiley-Interscience, 1971) (cit. on p. 19).

[111] V. Deitz and D. H. Andrews, "The symmetry of the benzene molecule", J. Chem. Phys **1**, 62–67 (1933) (cit. on p. 19).

[112] I. Barth, J. Manz, Y. Shigeta, and K. Yagi, "Unidirectional electronic ring current driven by a few cycle circularly polarized pulse: quantum model simulations for Mg-Porphyrin", J. Am. Chem. Soc. **128**, 7043–7049 (2006) (cit. on pp. 24, 30).

[113] C. Leforestier, R. H. Bisseling, C. Cerjan, M. D. Feit, R. Friesner, A. Guldberg, A. Hammerich, G. Jolicard, W. Karrlein, H.-D. Meyer, N. Lipkin, O. Roncero, and R. Kosloff, "A comparison of different propagation schemes for the time dependent Schrödinger equation", J. Compu. Phys. **94**, 59–80 (1991) (cit. on p. 29).

[114] S. Blanes and P. C. Moan, "Practical symplectic partitioned Runge-Kutta and Runge-Kutta-Nyström methods", J. Comput. Appl. Math. **142**, 313–330 (2002) (cit. on p. 29).

[115] S. Blanes and P. C. Moan, "Splitting methods for the time-dependent Schrödinger equation", Phys. Lett. A **265**, 35–42 (2000) (cit. on p. 29).

[116] T. J. Park and J. C. Light, "Unitary quantum time evolution by iterative lanczos reduction", J. Chem. Phys. **85**, 5870 (1986) (cit. on p. 29).

[117] H. Tal-Ezer and R. Kosloff, "An accurate and efficient scheme for propagating the time dependent Schrödinger equation", J. Chem. Phys. **81**, 3967 (1984) (cit. on p. 29).

[118] I. Barth, H.-C. Hege, H. Ikeda, A. Kenfack, M. Koppitz, J. Manz, F. Marquardt, and G. K. Paramonov, "Concerted quantum effects of electronic and nuclear fluxes in molecules", Chem. Phys. Lett. **481**, 118–123 (2009) (cit. on p. 170).

[119] A. Kenfack, I. Barth, F. Marquardt, and B. Paulus, "Molecular isotopic effects on coupled electronic and nuclear fluxes", Phys. Rev. A: At., Mol., Opt. Phys. **82**, 062502 (2010) (cit. on p. 170).

[120] H.-C. Hege, J. Manz, F. Marquardt, B. Paulus, and A. Schild, "Electron flux during pericyclic reactions in the tunneling limit: quantum simulation for cyclooctatetraene", Chem. Phys. **376**, 46–55 (2010) (cit. on p. 170).

[121] D. Andrae, I. Barth, T. Bredtmann, H.-C. Hege, J. Manz, F. Marquardt, and B. Paulus, "Electronic quantum fluxes during pericyclic reactions exemplified for the cope rearrangement of semibullvalene", J. Phys. Chem. B **115**, 5476–5483 (2011) (cit. on p. 170).

[122] T. Bredtmann, E. Hupf, and B. Paulus, "Electronic fluxes during large amplitude vibrations of single, double and triple bonds", Phys. Chem. Chem. Phys. **14**, 15494–15501 (2012) (cit. on p. 170).

[123] G. Hermann, B. Paulus, J. F. Pérez-Torres, and V. Pohl, "Electronic and nuclear flux densities in the H_2 molecule", Phys. Rev. A: At., Mol., Opt. Phys. **89**, 052504 (2014) (cit. on p. 170).

Acknowledgment

At the moment of finishing my doctorate study in Freie Universität Berlin, I am very appreciate for all people I met and all experience I had during these three and half years.

First of all, I would like to express my most gratefulness to Prof. Dr. Jörn Manz. I consider he is my enlightenment teacher in research field of quantum dynamics and he also suggested the topic of my PhD thesis. He is always kind, patient and helpful. He helps me really a lot in science as well as the life in Berlin, together with his dear wife - Etsuko. He brought me the motivation to continue my PhD study in abroad. He also helped me to have a chance to study here in a very good theoretical chemistry group of Prof. Dr. Beate Paulus.

Secondly, I would like to express my much grateful to my supervisor Prof. Dr. Beate Paulus for offering me the oppertunity to study in her group at a nice work place, and for creating a very international, friendly group atmosphere. She was also very supportive for my study here, from the beginning to the end.

Thirdly, I would like to give lots of thanks to my supervisor Prof. Dr. Jean Christophe Tremblay. He is always so nice and taught me much about the simulation methods and skills. I am very lucky to have him as my PhD supervisor. I am also very thankful to him for reading and correcting my PhD thesis.

I also would like to thank all previous and current members in the AG Paulus, especially Prof. Dr. Jhon Fredy Pérez-Torres, Dr. Vincent Pohl, Dr. Gunter Hermann for introducing me into various efficient methods and for great cooperation and also to Dr. Matthias Berg, Christian Stemmle for kindly help.

I also thank the experimental partners Prof. Dr. Kenji Ohmori, Prof. Dr. Nobuyuki Takei, Dr. Yichi Zhang and Dr. Christian Sommer for carrying out a proof-in-principle experiment which confirms our theoretical prediction in this thesis for ^{87}Rb atom with ± 3 attoseconds precision.

I would also like to express much thanks to China Scholarship Council for financial support for doing my PhD.

I also want to thank all my good friends make me a happy and memorable life in Berlin. Thanks for their accompany and help.

Finally, I want to thank very much my beloved family. Their support and understanding give me the best state and make me concentrate on studying here.